M-PM-A1 ARE THE CONCEPTS USED TO DESCRIBE ENZYME ACTION CONSISTENT? D.N. Jacobson* (Intr. by M.R. Adelman), Duke University, Durham, North Carolina 27710

It is argued that there is an inconsistency between three concepts which are generally thought to apply to enzyme action. One is the requirement, imposed by the second law of thermodynamics, that the presence of an enzyme not change the equilibrium constant of a chemical reaction and, therefore, for a reversible reaction at thermodynamic equilibrium, that enzyme catalysis must increase the rates of the forward and reverse reactions to the same degree. The second is the idea that the conformation of an enzyme-substrate complex may depend on the precise structure of the bound substrate. The third is the concept that the rate limiting step of a chemical reaction, either free in solution or catalyzed by an enzyme, is passage of the complex of reacting atoms through a high energy transition state, with a structure different from that of either starting or product reactants. The catalytic effectiveness of an enzyme depends on a similarity between the ground and transition state enzyme-substrate complexes. However, the difference between the structures of the starting and product reactants means that there is no necessary relationship between the conformations of the complexes formed by an enzyme with starting or product substrates. Moreover, once the transition state has been passed, changes in substrate structure can induce a change in the conformation of the enzyme-substrate complex to one unfavorable for the reverse reaction without affecting the rate of the forward reaction. Therefore, there appears to be no necessity for enzymes to have an equal effect on forward and reverse reactions.

M-PM-A2 STUDIES OF THE ACTIVE SITE LYSINE OF RIBONUCLEASE A BY ^{13}C NMR. J.E. Jentoft* T. A. Gerken*, N. Jentoft*, D.G. Dearborn, Case Western Reserve University, Cleveland, Ohio 44106

The free amino groups of ribonuclease A were reductively methylated with $NaCNBH_3$ and ^{13}C-enriched formaldehyde (Jentoft et al., J. Biol. Chem., in press). A specific NMR signal has been assigned to lysine 41, a residue in the active site of ribonuclease. The rationale for the assignment is (1) the pKa of the residue is 9.0, corresponding closely to the pKa of 8.8 previously assigned by others to this residue; (2) enzyme activity is lost in parallel with modification of this group; and (3) this residue can be protected by inhibitors during modification with a corresponding partial protection of enzyme activity. The pH behavior of the methylated lysine 41 has been determined in the presence and absence of saturating concentrations of ribonuclease inhibitors. Cytidine monophosphate inhibitors behave identically, causing a shift in the pKa of lysine 41 to 9.11, while phosphate and sulfate, which also inhibit, cause a larger shift in the pKa, to 9.27. Cytidine, which lacks the phosphate group, causes a change identical to that of the cytidine monophosphate inhibitors. These results demonstrate that changes in the pKa of lysine 41 may be caused not only by the phosphate moiety (phosphate and sulfate results), but also by some other functional group(s) since cytidine causes the same changes in pKa as the cytidine monophosphates. The magnitude of chemical shift changes during titration of lysine 41 also varies with inhibitor, and these variations as well as studies with other inhibitors will be discussed in relation to a role for lysine 41 in the mechanisms of action of ribonuclease.

M-PM-A3 LAC REPRESSOR: NUCLEAR MAGNETIC RELAXATION TIMES. Mary Ann Jarema and Ponzy Lu, Department of Chemistry, University of Pennsylvania, Philadelphia, Pennsylvania 19104.

The Lac Repressor is a tetrameric protein composed of identical subunits of 360 amino acids each with a total molecular weight of 154,360. We have isolated this protein with 3-fluorotyrosine in each of its 8 tyrosines and are undertaking a NMR study of its structure and function using Fluorine-19 as a nuclear spin label. The logitudinal relaxation times of the fluorines have been measured by progressive saturation, inversion recovery and by dynamic decoupling techniques. The latter technique involved measuring the nuclear Overhauser enhancement upon double irradiation of the protons. We observe a variation of -0.5 to -1 in the nuclear Overhauser enhancements for the various tyrosine positions, indicating segmental mobility of parts of the molecule. The NMR data is in qualitative agreement with biochemical studies. Since we are able to assign the resonances through genetic methods, it is possible to relate this data to specific points in the primary sequence. (Supported by grants from NIH and the American Cancer Society)

M-PM-A4 STRUCTURAL INFLUENCE OF TYROSYL IODINATION IN PROTEINS BY CIRCULAR DICHROISM SPECTROSCOPY. Alan G. Walton and Frances I. Hurwitz* Case Western Reserve University, Cleveland, Ohio 44106.

Iodination of tyrosine residues in proteins depends upon the accessibility of the residue to the aqueous environment; thus mono-, di- or non-iodinated residues may result. If all of the tyrosyl residues are halogenated the ultraviolet absorbance bands are moved to increasing wavelength and their contribution to circular dichroism spectra may be evaluated. Three classes of iodinated proteins will be reported, the first pertaining to proteins with normally anomalous C.D. spectra and known three-dimensional structure (e.g. bovine pancreatic trypsin inhibitor). The second class is that of C.D. "normal" proteins with known structure (e.g. myoglobin, lysozyme) and the third that of proteins of unknown structure (e.g. bovine serum albumin and fibrinogen). In these examples there is an interplay between degree of iodination, residue accessibility, conformation changes and the resolution of these changes by circular dichroism spectroscopy. Anomalous spectra can arise from the electronic environment of only one tyrosyl residue (B.P.T.I.) and iodination has the effect of reducing the pK of the tyrosyl moiety such that the diiodinated species is generally deprotonated at neutral pH. Consequently the diiodo-tyrosine residue seeks a more hydrophilic environment than its non-iodinated counterpart, an effect which destabilizes the structure and often modifies it slightly.

M-PM-A5 FLUORESCENCE STUDIES OF CYTOCHROME C CONFORMATIONS AT LOW pH. B.F. Peterman and K.J. Laidler*, Department of Chemistry, University of Ottawa, Ottawa, Ontario, Canada K1N 9B4.

Fluorescence properties of acid unfolded cytochrome c (pH 1.6) were examined. Reliable tyrosine and tryptophan emission spectra are only obtained if corrections are made for reabsorption by the heme group. By measuring the lifetime of the excited state of the single tryptophan residue in cytochrome c and apocytochrome c, we were able to estimate the energy transfer from the Trp 59 to the heme group. This allowed us to calculate a value of 40 A for the distance between Trp 59 and the heme group at pH 1.6. From the intrinsic viscosity of cytochrome c at pH 1.6 we estimated a value of 38 A for the distance between Trp 59 and the heme group, in good agreement with the energy transfer measurements. The results of both viscosity and energy transfer measurements indicate that at pH 1.6, cytochrome c assumes a linear random coil conformation.

Fluorescence quenching, which arises from the increased nonradiative energy transfer from tyrosines and tryptophan to the heme group, was employed to follow the folding of various portions of the polypeptide chain under the influence of increased salt concentration. The results suggest that the part of the polypeptide chain containing Trp 59 approaches the heme group more closely than the portion of the chain near the C - terminal.

M-PM-A6 Cu^{2+}- GLYCOSAMINOGLYCAN-COMPLEX SPECTRA AS A PROBE TO STUDY Ca^{2+} - GLYCOSAMINOGLYCAN BINDING. J.W. Park, D.C. Mukherjee,* and B. Chakrabarti, Eye Research Institute of Retina Foundation, Boston, Mass. 02114.

Control of osmotic pressure in a tissue and transport of metal ions across a tissue are determined mainly by the interaction properties of the polymer with ions. Chondroitin 4-sulfate in cartilage with proteoglycan has been shown to provide sites for Ca^{2+} deposition during calcification. The proposed function of cell-surface glycosaminoglycans (GAG) in relation to certain aspects of cell behavior, including growth and differentiation, was also related to Ca^{2+} binding activities. Utilizing a characteristic absorption band at 237 nm of the Cu^{2+}-GAG complex, the binding constants of Cu^{2+} and Ca^{2+} to heparin, dermatan sulfate, and chondroitin sulfate have been determined spectroscopically. The order of binding constant for both ions is heparin > dermatan sulfate > chondroitin sulfate. Affinities for both ions to chondroitin sulfate do not differ much, but a 2- to 3-fold higher affinity for Cu^{2+} than for Ca^{2+} is obtained for heparin and dermatan sulfate. These results are explained as chelation of both carboxyl and sulfate groups to Cu^{2+} in heparin and dermatan sulfate, but not in chondroitin sulfate. The logarithm of binding constants varies linearly with the square root of the ionic strength, indicating that the electrostatic forces are the predominant factor in the metal-ion interaction with glycosaminoglycans. High binding constants of Ca^{2+} to heparin and dermatan sulfate are related to the observations of the parallelism between the Ca^{2+} and sulfated glycosaminoglycan contents of the cell coat, and the decreased amount of high Ca^{2+} binding glycosaminoglycans, heparan sulfate, and dermatan sulfate, in neonate and tumoral tissues.

M-PM-A7 GLYCOPROTEIN CONFORMATION IN THE REGION OF CARBOHYDRATE LINKAGE TO ASPARIGINE. C. Allen Bush

The conformation of the glycopeptide linkage region of the serum type glycoproteins has been studied by CD and NMR experiments on the linkage compound, 2-acetamido-1-N-(4-L-aspartyl)2-deoxy-β-D glucopyranosyl amine. In the proposed model, the peptide chain forms a type I β-turn. The conformation of the carbohydrate linkage is specified by the asparagine side chain dihedral angles X_1 and X_2 and by ϕ_1, the dihedral angle about the glycosyl amide bond linking asparagine to N-acetyl glucosamine.

The CD spectrum of β-Asn-GlcNac in the 170-210 nm region is particularly sensitive to ϕ_1 as a result of exciton coupling between the linkage amide and that of the 2-acetamido sugar. A detailed theory of the CD of vicinal diacyl amino sugars is used to relate experimental CD spectra to the amide dihedral angles.

Proton NMR experiments have been used to measure the vicinal coupling constants of the amide protons. The amide dihedral angles, determined from these data by means of a Karplus relation commonly used in peptide NMR studies, are consistent with those determined by CD experiments. Vicinal H-H and C-H coupling constants of the side chain protons give information on X_1. The proposed model based on these data features a hydrogen bond from the proton of the linkage amide to the peptide oxygen of the asparagine residue. (Supported by NSF Grant CHE 76-16783.)

M-PM-A8 BIOLOGICAL FUNCTION OF GRAMICIDIN: COMPARISON OF THE EFFECT OF LINEAR GRAMICIDIN ANALOGS ON MEMBRANE PERMEABILITY, BACTERIAL SPORULATION, AND RNA POLYMERASE. W. Veatch, Department of Pharmacology, and N. Sarkar*, P.K. Mukherjee*, D. Langley*, and H. Paulus*, Department of Biological Chemistry, Harvard Medical School, Boston, Mass. 02115.

Gramicidin is a linear polypeptide antibiotic produced by Bacillus brevis at the onset of sporulation. A mutant has previously been isolated which does not biosynthesize gramicidin, and does not sporulate properly. However, addition of exogenous gramicidin restores the normal spore phenotype, thereby demonstrating a biological function for gramicidin.

Various analogs of linear gramicidin were tested for their biological activity in restoring the normal spore phenotype of these mutants and for their ability to increase cation conductivity of black lipid membranes and to inhibit bacterial RNA polymerase in vitro. Whereas many biologically active gramicidin analogs had no effect on membrane permeability, all biologically active peptides were able to inhibit RNA polymerase. These observations exclude membranes as the site of action of gramicidin during bacterial sporulation but are consistent with the notion that gramicidin functions to control RNA synthesis during the transition from vegetative growth to sporulation. The relationship between peptide structure and the ability to restore normal sporulation and inhibit RNA polymerase showed that the eight amino terminal residues have little influence on the function of gramicidin whereas the highly nonpolar repeating sequence $(\text{D-Leucyl-L-Tryptophan})_4$ is essential for biological activity and represents the site of interaction with RNA polymerase. Because gramicidin inhibits RNA polymerase by binding competitively with the double stranded DNA template (Sarkar, Langley & Paulus), a model for the C-terminal half of gramicidin is proposed which bears a striking resemblance to one chain of a DNA double helix, with the four tryptophan indoles in place of the bases.

M-PM-A9 COLLAGEN FIBRIL FORMATION: THE ROLE OF THE NON-HELICAL TERMINAL REGIONS. R. A. Gelman, D. C. Poppke* and K. A. Piez*. National Institute of Dental Research, NIH, Bethesda, MD 20014.

Fibril formation was initiated by diluting a cold acid solution of collagen monomer (triple helical), derived from rat tail tendon, with a NaCl-TES-phosphate buffer, pH 7.3, and raising the temperature; the process was monitored by turbidity and electron microscopy. Normal collagen forms native-banded fibrils in a multistep process. Early stages are dominated by linear assembly and late stages by lateral assembly. Reduced collagen, with the non-helical ends intact but unable to form covalent crosslinks, assembles with a half-time which is less than two-fold greater than normal collagen. The decreased rate can be explained by increased reversibility of the late stages of assembly. The fibrils are indistinguishable from those made by normal collagen. Removal of the non-helical terminal region of the protein by pepsin digestion results in a half-time of assembly which, compared to normal collagen, is increased ∿13-fold. Kinetic data indicates that although the overall mechanism is quite similar, there may be some differences in the early stages of assembly. The fibrils are not well ordered and are much shorter than those formed from normal collagen. We conclude that the non-helical ends participate in the regulation of the rate of assembly and structure of the product through specific non-covalent interactions.

M-PM-A10 FACTORS AFFECTING ELASTIN CALCIFICATION. Marianna M. Long, Dan W. Urry, John R. Baker* and Bruce Caterson*, Laboratory of Molecular Biophysics, University of Alabama Medical Center, Birmingham, Alabama 35294.

The elastic fiber is a major focus for arterial wall calcification and lipid deposition. Its precursor protein is tropoelastin which contains repeating peptides, a tetramer Val-Pro-Gly-Gly, a pentamer Val-Pro-Gly-Val-Gly, and a hexamer Ala-Pro-Gly-Val-Gly-Val. Calcium titrations of these peptides demonstrate their different binding affinities. The ratios of the affinities are 1:1.6:1.3:2.5 for the pentamer, polypentamer, hexamer and polyhexamers, respectively. Cross-linked polypentamer calcified in bovine serum uniformly while the polyhexamer calcified only in isolated areas. These data support the conclusion that intrinsic factors (e.g. primary structure and the resultant conformation) can affect both calcium binding and calcification of the elastin molecule. The microfibrillar glycoprotein sheath of the elastic fiber could afford extrinsic control by shielding the elastin from calcium ions. Temperature profiles of coacervation with well characterized bovine nasal cartilage proteoglycan and elastin peptides show that the polypentamer does not interact while the polyhexamer does, suggesting specific sites for elastin-proteoglycan and possibly by analogy elastin-glycoprotein interactions.

M-PM-A11 SOLVENT DENATURATION IN HYALURONATE SOLUTIONS. T.W. Barrett, University of Tennessee Center for the Health Sciences, Memphis, TN 38163.

The thermodynamic analysis of solvent denaturation by Schellman (Biopolymers 17 (1978) 1305) is applied to the abrupt conformational transition occuring in hyaluronate solutions buffered in phosphate (Barrett & Harrington, Biopolymers 16 (1977) 2167; Barrett, Biopolymers 17 (1978) 1567). The transition is described in terms of a thermodynamic binding parameter, Γ_{32}, which is the equivalent of the stoichiometric binding parameter in site-binding theory, but which includes all modes of interaction of the molecule with the solvent including stoichiometric binding. This difference enables the treatment of long-range interaction and counter-ion condensation effects on the apparent pK of hyaluronate solutions.

The ability of phosphate buffers to shift the pK_a of hyaluronate solutions far from the pK_o is due to the demonstrated tendency of neutralized alkali groups - such as the amide groups - and phosphate ions to site bind, as opposed to atmosphere bind. As the abrupt conformational transition is accompanied by an equally abrupt change in the second virial coefficient, it is suggested that the transition is due to a change of control from site binding to ionic atmosphere binding, when the average axial distance between polyelectrolyte groups falls below 7 Å. In solutions in which the electrolytes are less able to penetrate the hydration shell of the amide group, the pK_a is less removed from the pK_o and consequently the change of control occurs at a lower pH.

M-PM-A12 ASSOCIATION CONSTANTS OF LINEAR PEPTIDES BY VAPOR PRESSURE OSMOMETRY. E. S. Stevens and N. Sugawara,* State University of New York, Binghamton, N.Y. 13901

Association constants have been measured in chloroform for peptides of the type t-Boc-Gly-L-Val-Gly-OMe, Ac-L-Val-Gly-OMe, t-Boc-L-Nva-OMe, Ac-L-Nva-OMe, and others, by vapor pressure osmometry. The results are applied to the interpretation of the temperature dependence of NH chemical shifts measured at 270 MHz.

M-PM-A13 KINETICS AND MECHANISMS OF NO_x AND O_x POLLUTANT METABOLISM IN WHOLE BLOOD. George D. Case and Paul J. Bekowies*, Energy & Environment Division, Lawrence Berkeley Laboratory, University of California, Berkeley, CA 94720; and Analytical & Supporting Research Division, Morgantown Energy Technology Center, U.S. Department of Energy, Morgantown, WV 26505 # (#, present address of both authors).

The kinetics and mechanisms of NO, NO_2, NO_2^-, and O_3 metabolism in whole blood were investigated *in vitro* and *in vivo*. O_3 does not react to any detectable extent with any metalloprotein in blood. Nitrogenous species (under aerobic conditions) stoichiometrically convert hemoglobin derivatives ultimately to methemoglobin (Hb'''). A computer model using various literature and experimental rate constants was used to establish a mechanism for the reactions of NO, NO_2, and NO_2^- with deoxyhemoglobin (Hb") and oxyhemoglobin (HbO_2). The results suggest that oxidation of a T-state hemoglobin derivative generates an S=1/2 form of Hb''' exclusively (Spin states measured by EPR at 19K). Conversely, oxidation of an R-state hemoglobin derivative produces an S=5/2 Hb''' exclusively. The present results do not necessarily conflict with earlier reports (Perutz, 1972; Gibson & coworkers, 1976,1977) correlating R:T distributions with spin states of Hb''' products, since the spin state is very sensitive to measurement temperature as well as tertiary and quaternary protein structure. Under typical environmental exposure conditions, oxidation of HbO_2 to S=5/2 Hb''' occurs *in vivo* to a significant and potentially dangerous extent due to NO and NO_2 present in air and/or to NO_2^- in food or water sources. Hb''' body burden analysis appears to represent a reasonably quantitative and rapid bioassay screening procedure for human exposures to oxides of nitrogen. This work was supported under the auspices of the U.S. Energy Research & Development Administration and the U.S. Department of Energy.

M-PM-A14 SOME ELASTIC PROPERTIES OF HAIR AND THE DISEASE ARGINOSUCCINICACIDURIA. Anthony A. Silvidi, Biophysics Lab., Physics Dept., Kent State Univ., Kent, Ohio 44242, and Joseph L. Potter,* Dept. of Pathology, Children's Hospital Medical Center, Akron, Ohio 44308.

Stress-strain characteristics and amino acid content of hair from a child with the disease arginosuccinicaciduria have been compared with normal hair over a period of approximately eight years. The disease which is associated with mental retardation, epilepsy, ataxia, and liver disorder is a rare inborn error of metabolism. Young's modulus, tensile strength and the percent change in length of hair at the break point for the patient and controls will be presented. It will be shown that while these characteristics were below normal values at the beginning of the measurement period as the child grew toward puberty they were moving back toward normal values. Correlation between these physical parameters and amino acid content of the hair will also be shown.

M-PM-B1 MOTION AND ORDER IN THE GEL STATE OF BIOLOGICAL MEMBRANE LIPID AS SEEN BY ^2H NMR. Ian C.P. Smith, K.W. Butler, P. Tulloch*, M. Bloom*, and J.H. Davis*, Div. Biol. Sci., NRC, Ottawa, Canada K1A OR6 and Dept. Phys., UBC, Vancouver, Canada V6T 1W5.

^2H NMR has been widely applied to model membrane systems. However, detailed application to a biological membrane has only been accomplished with A. laidlawii (1). Until recently only the spectra of liquid crystalline lipid has been readily observable, that of gel state lipid remaining invisible due to short T_2 values and large spectral widths. Using the quadrupole echo technique (2) we have followed the temperature dependence of the ^2H NMR spectra of specifically-deuterated palmitoyl chains in the membranes of A. laidlawii over the range 0-55°C. Even at temperatures above that of the onset of the calorimetrically-determined liquid crystal-gel state transition, detectable amounts of more rigid and more ordered lipid are present; the population of rigid lipid increases rapidly with decreasing temperature thereafter. However, over the entire range of the membrane phase transition both states of the lipid are observed, and the rate of exchange of lipid between them must be less than 3×10^4 s^{-1}. Upon completion of the enthalpic transition the palmitoyl chains are highly ordered, but retain a rapid axial motion. Further cooling from 20-0°C results in cessation of this rapid motion and the appearance of a spectrum with a quadrupole splitting of ca. 120 kHz. Thus, at 5°C the membrane lipids are truly solid. The behaviour inferred from the ^2H quadrupole splittings was also manifest in the temperature dependence of the second moment of the ^2H spectrum. The implications of the coexistence of two lipid phases at the growth temperature will be discussed.

1. Stockton et al., Nature 269, 267 (1977).
2. Davis et al., Chem. Phys. Lett. 42, 390 (1976).

M-PM-B2 ORIENTATIONAL ORDER AND CONFORMATION OF THE HEAD GROUP IN THE BILAYER MEMBRANE, J.W. Doane* and M.J. Vaz* (Intr. by F. Walz), Kent State University, Kent, Ohio 44242.

An order parameter-based interpretation is applied to the temperature dependence of the deuterium magnetic resonance splittings and the anisotropic contribution to the chemical shift for ^{31}P from the head group of 1,2-dipalmitoyl-sn-glycero-3-phosphocholine (DPPC). It is shown that the molecular long axis is a twofold rotation axis instead of an axis for free rotation as normally assumed. Furthermore, the data are shown to be entirely consistent with the presence of three orientational order parameters and that the head group undergoes little change in its conformation as the temperature is varied even as the liquid crystal-gel phase transition is transversed. Finally, it is shown that the temperature dependence of the anisotropic contribution to the chemical shift for ^{31}P can be predicted from that of the deuterium quadrupole splittings.

M-PM-B3 SPHINGOMYELIN AND LECITHIN BILAYERS AND THEIR INTERACTION WITH CHOLESTEROL, W.I. Calhoun* and G.G. Shipley, Biophysics Division, Boston University School of Medicine, Boston, Ma., 02118.

Aqueous dispersions of N-palmitoyl sphingomyelin (PSM) were examined by differential scanning calorimetry (DSC) and x-ray diffraction. PSM undergoes an endothermic gel-liquid crystalline transition (ΔH = 5.8 Kcal/mole) at 40.5°C. At 10°C, x-ray diffraction of a PSM:H_2O (50:50 w/w) dispersion showed that the structure was lamellar, with a limiting bilayer repeat distance of 77.8 Å. The hydrocarbon chains are probably tilted with respect to the bilayer normal. At 50°C, above the transition, the structure remains lamellar, the bilayer repeat distance decreasing to 61.6 Å. PSM and dimyristoyl lecithin (DML) were shown to be miscible in both the gel and liquid-crystalline phase by DSC and x-ray diffraction and no lateral phase separation occurs. The addition of various amounts of cholesterol to PSM bilayers and DML bilayers produced similar effects as monitored by calorimetry; the sharp order-disorder transition decreased in enthalpy and was not observable at 25 mole% cholesterol. As cholesterol was added, a broad transition appeared with a peak maximum at a temperature slightly higher than that of the sharp component. This transition is the only transition observeable at 25 mole% cholesterol. This transition becomes progressively broader and is no longer visible at ~42 mole% cholesterol. When increasing amounts of cholesterol were added to an equimolar mixture of PSM and DML, the peak temperature of the residual sharp transition (32°C) remained unchanged up to 25 mole% cholesterol. On this basis we conclude that the sterol has no preferential affinity for either phospholipid and that the interaction is very similar to that of the PSM-cholesterol and DML-cholesterol systems.

M-PM-B4 MEASUREMENT OF ANISOTROPIC TWO-DIMENSIONAL LATERAL TRANSPORT IN MEMBRANES BY FOURIER ANALYSIS OF TWO-DIMENSIONAL PERIODIC PHOTOBLEACHED PATTERNS. Barton A. Smith and Harden M. McConnell, Chem. Dept., Stanford Univ., Stanford, CA 94305, and William R. Clark,* Molecular Biology Institute, Univ. of Calif., Los Angeles, CA 90024.

We have extended the technique of fluorescence redistribution after pattern photobleaching[1] to the analysis of two-dimensional transport processes in which the transport may be directionally anisotropic. This new method makes possible the simultaneous measurement of different diffusion coefficients for different directions. Fluorescent molecules in the sample are photobleached in a pattern which is periodic in two perpendicular directions. Fluorescence photomicrographs of the sample taken at time intervals after photobleaching are Fourier analysed. The redistribution of fluorescent molecules causes a decay with time of the Fourier amplitudes corresponding to the spatial frequencies present in the original pattern. For example, diffusion of the fluorescent molecules causes an exponential decay of the Fourier amplitudes, and diffusion coefficients for the two perpendicular directions can be calculated from the characteristic decay times of these amplitudes. In addition, other types of transport can be identified and characterized by examination of the Fourier spectrum. We have applied the above method to the search for anisotropic diffusion of protein molecules on the surfaces of living cells. Some results of these studies will be briefly presented, and will be discussed in more detail in another paper to be presented at this meeting.

1. B. A. Smith and H. M. McConnell, Proc. Natl. Acad. Sci. USA 75, 2795-2763 (1978).

This work has been supported by the National Science Foundation Grant PCM 77-23586. B. A. Smith is a National Science Foundation Postdoctoral Fellow.

M-PM-B5 SURFACE DIFFUSION OF CYTOCHROMES C AND C2. R.E. Overfield* and C.A. Wraight, Department of Physiology and Biophysics, University of Illinois, Urbana, Illinois 61801

The photooxidation of equine cytochrome c and bacterial cytochrome c2 by isolated reaction centers from Rp. sphaeroides (R-26) in free solution is second order. The net forward rate constants (k') in 10 mM Tris at pH 8.0 were 5×10^9 and 8×10^8 M^{-1} sec^{-1} respectively and decreased with ionic strength. Cytochrome c2 oxidation was biphasic; a 2 μs phase was 30% of the total when the second order phase limited at 400 μs. In vivo kinetics were resolved to two phases of equal magnitude with $t_{\frac{1}{2}}$ = 3 μs and 200 μs. Photooxidation of the cytochromes by reaction centers incorporated into neutral unilammellar vesicles of egg phosphatidylcholine gave similar results except that k' was reduced by a factor of two. When the reaction centers were incorporated into negatively charged phosphatidylserine vesicles the reaction remained first order in cytochrome and first order in reaction centers at high cyt:RC ratios, but became zero order in reaction centers at low cyt:RC ratios. The diffusion controlled rate constant for cytochrome c2 on PS vesicles was 1×10^8 M^{-1} sec^{-1} and increased with ionic strength. In 0.1 M NaCl, k' was five fold faster in negative vesicles than in neutral ones, but the activation energy remained 8-9 kcal/mole. The negative surface charge also increased the proportion of fast phase. Two-dimensional diffusion of the cytochrome on the membrane surface is proposed to account for these results. At low cyt:RC ratios, increasing the ionic strength enhanced the extent of oxidation indicating an increased diffusion length. Approximate values for this parameter (Eigen: $\sqrt{D2/kdiss}$) at low ionic strength and in 0.1 M NaCl are 30 Å and 150 Å for cytochrome c and 150 Å and >250 Å for cytochrome c2. Supported by NSF PCM 77-25725. R.E.O. was an NIH trainee.

M-PM-B6 ANISOTROPIC DIFFUSION OF PROTEINS IN CELL MEMBRANES. Barton A. Smith and Harden M. McConnell, Chemistry Department, Stanford University, Stanford, CA 94305, and William R. Clark,* Molecular Biology Institute, University of California, Los Angeles, CA 90024.

At the 1978 Annual Meeting of the Biophysical Society, Dr. S. J. Singer postulated that certain membrane components in fibroblasts and other flattened cells grown in monolayer culture would exhibit anisotropic diffusion due to the interaction of these membrane components with intracellular stress fibers containing actin and myosin.[1] We have developed a technique for the characterization of two-dimensional motion which makes possible the detection of anisotropic diffusion on cell surfaces, and have applied this technique to the study of the motion of Concanavalin A receptors on living fibroblasts. We use Fourier analysis of the distribution of fluorescence on cells which have been photobleached in a two-dimensional periodic pattern to study the motion of fluorescent molecules on the cell surface. Balb·b mouse embryo fibroblasts grown on plastic tissue culture dishes were stained with fluorescein-labeled succinyl Con A. Motion of the fluorescent molecules was monitored at room temperature. We have observed significant anisotropy in the motion of these molecules, with the motion being much faster in the direction parallel to the expected direction of actin-myosin stress fibers. Further studies are in progress on this and other systems. The details of the experimental technique will be presented elsewhere at this meeting.

1. S. J. Singer, et al., Biophysical J. 21, 78a (1978).

This work has been supported by the National Institues of Health Grant 5R01 AI13587 and the American Cancer Society Grant IM-48. BAS is a National Science Foundation Postdoctoral Fellow.

M-PM-B7 RATE OF LATERAL DIFFUSION OF M13 COAT PROTEIN IN MODEL MEMBRANES. Lloyd M. Smith and Harden M. McConnell, Chem. Dept., Stanford Univ., Stanford, CA 94305.

A fluorescent derivative of the M13 phage coat protein has been reconstituted into oriented lipid multilayers, and its rate of lateral diffusion determined by the FRAPP[1] method. In the fluid phase of dimyristoyl phosphatidylcholine multilayers the rate of diffusion is of the same order of magnitude as that of the lipid. As one cools the sample below the main transition temperature, previously oriented regions become distorted and the fluorescence becomes non-uniform. This change is reversible and is probably due to aggregation of the protein. Quantitative data will be presented for the region above the phase transition temperature, and the effects of cholesterol and cardiolipin examined. This is the first measurement of the rate of diffusion of a protein reconstituted into a well-defined model membrane.

1. B. A. Smith and H. M. McConnell, Proc. Natl. Acad. Sci. USA 75, 2795-2763 (1978).
This research has been supported by the National Science Foundation Grant 77-23586. LMS is a trainee under the National Institutes of Health Cellular and Molecular Training Grant GM 7276.

M-PM-B8 FLUORESCENCE ANISOTROPY MEASUREMENTS UNDER OXYGEN QUENCHING CONDITIONS FOR THE QUANTITATION OF THE DEPOLARIZING ROTATIONS OF FLUOROPHORES. F. G. Prendergast and J. R. Lakowicz, Dept. of Pharmacology, Mayo Foundation, Rochester, MN and Dept. of Biochemistry, Gray Institute, Univ. of Minnesota, Navarre, MN.

The Perrin-Weber equation shows that there is an inverse relationship between fluorescence anisotropy and fluorescence lifetime. By varying the fluorescence lifetime and simultaneously measuring anisotropy it should therefore be possible to determine the rotational rate of fluorophores in isotropic solvents. In situations where the motion of the probe is hindered, we have obtained the following relation from Weber's equations $r = r_\infty + \frac{r_o - r}{6R\tau}$. The parameter r_∞ provides a measure of the degree to which the fluorophore's environment hinders its rotational diffusion. We have measured the fluorescence anisotropy of diphenylhexatriene (DPH) as its fluorescence lifetime is decreased by oxygen quenching. Such studies were done on DPH dissolved in mineral oil and for DPH embedded in phospholipid vesicles. The data show that the values obtained for the rotational rate (R) of DPH in mineral oil agree precisely with those obtained from steady state anisotropy measurements and differential phase fluorometry -- r_∞ was found to be zero. In contrast, DPH embedded in vesicles of dimyristoylphosphatidylcholine (DMPC), behaves as an isotropic but highly hindered rotator (r_∞ = 0.33). Additionally, the data were used to calculate microviscosities ($\bar{\eta}$) of bilayers and revealed broad disparities in $\bar{\eta}$ of bilayers as measured by three different fluorescence methods. For example, at 5°C in DMPC vesicles, the microviscosities as determined from measurements of steady state anisotropies and oxygen diffusivity are 50 and 0.3 poise respectively. These disparities indicate that the apparent microviscosity of lipid bilayers is highly dependent upon the process used in its estimation. Supported by Grant ES 01283 of USPHS (to JRL) and MDA-24 (to FGP).

M-PM-B9 EFFECTIVE POLARITY OF THE INTERIOR OF ARTIFICIAL MEMBRANES PROBED BY THE FLUOROPHORE PYRENE. P. Lianos* and S. Georghiou, Univ. of Tennessee, Dept. of Physics, Knoxville, TN 37916.

The strong dependence of the structure of the fluorescence spectrum of pyrene on the polarity of its environment has been shown by statistical analysis of the fluorescence decay profiles and by infrared spectroscopy to be the result of complex formation between pyrene and polar groups which causes a reduction in the symmetry of the pyrene molecule giving, in turn, rise to enhancement of weakly allowed vibronic transitions. A similar effect was also observed when pyrene is incorporated into egg-lecithin or L-a-lecithin vesicles. It is inferred that structural fluctuations allow extensive penetration of the water-lipid interface into the vesicles.

M-PM-B10 EFFECTS OF DIETARY FAT ON THE FLUIDITY OF PLATELET MEMBRANES. Elliott Berlin and Calvert Young,* Lipid Nutrition Laboratory, NI, SEA, USDA, Beltsville, Md. 20705

Dietary fat type is reflected in the phospholipid fatty acid composition of the plasma membrane of rabbit platelets, hence, controlling the fluidity of these membranes. Rabbits were maintained for six months on diets varying in stearic and polyunsaturated fatty acid contents to provide diets differing in thrombogenicity. Microviscosities at 37°C, calculated from the anisotropy of fluorescence from the probe 1,6-diphenyl-1,3,5-hexatriene were 3.46, 3.37, 2.32, and 2.16 poise for platelet membranes isolated from rabbits whose only source of dietary fat was cocoa butter, milkfat, coconut oil or corn oil, respectively. Values for ΔE, the energy of activation for fusion, were -6.63, -6.15, -6.09, and -7.47 kcal/mole for these same membranes, respectively. Measurements with intact platelets yielded η= 2.41 poise at 37°C and ΔE= -7.78 kcal/mole for cells isolated from cocoa butter fed rabbits. When rabbits consumed the other fats, η for the intact cells exceeded that of the corresponding membrane isolates with little difference between membrane and cellular ΔE values. Some of the differences between cell and membrane fluidities can be associated with fatty acid compositional distinctions, particularly with the rabbits fed cocoa butter. The increased fluidity and disorder of platelets from the cocoa butter fed rabbits might relate to the higher thrombogenicity of this fat. A significant rigidifying effect of a non-fatty acid diet component was noted with rabbits fed a commercial rabbit chow. Though the fatty acid compositions of the chow and corn oil were almost identical, values of η= 3.28 ± .41 poise at 37°C and ΔE= -7.29 ± .63 kcal/mole were observed with isolated platelet plasma membranes.

M-PM-B11 THE APPLICATION TO NITROXIDE SPIN LABELS OF ALKYLCOBALT PHOTOCHEMISTRY: A NEW METHODOLOGY FOR PROBLEMS IN MEMBRANE BIOPHYSICS. James R. Sheats and Harden M. McConnell, Dept. of Chemistry, Stanford University, Stanford, CA 94305.

The photochemical reaction of alkylcobalt complexes (e.g., alkylcobalamins, alkylpentacyanocobaltates)[1] with nitroxides has been shown to provide a unique and versatile method for the specific, controlled destruction of spin labels.[2,3] More recently the kinetics of this reaction have been analyzed and shown to be very sensitive to the dynamic environment of the nitroxide. Membrane studies involving both headgroup and hydrocarbon spin labels in dimyristoyl lecithin multilayers will be presented, illustrating applications to bilayer permeability and density fluctuations, and to the structure of lecithin-cholesterol mixtures.

1. J. R. Sheats and H. M. McConnell, J. Amer. Chem. Soc. 99, 7091-7092 (1977).
2. J. R. Sheats and H. M. McConnell, Proc. Natl. Acad. Sci. USA 75, Oct. 1978 (in press).
3. M. A. Schwartz and H. M. McConnell, Biochemistry 17, 837-840 (1978).

This research has been supported by the National Science Foundation Grant PCM 77-23587. JRS has been supported by a National Science Foundation Predoctoral Fellowship.

M-PM-B12 THE DETECTION OF RADICAL INTERMEDIATES IN THE ACTIVATION OF N-NITROSAMINES AND N-NITROSOUREAS USING SPIN-TRAPPING TECHNIQUES. W. B. Harrison*, R. A. Floyd, Oklahoma Medical Research Foundation, Oklahoma City, OK 73104.

Electron spin resonance spectroscopy has been employed to study the nature of the intermediates formed in the process of activation of N-nitrosamines, N-nitrosoureas, and N-nitrosoguanidines by a variety of microsomal systems. The technique of spin-trapping has been utilized to detect, isolate, and identify the nature of the radical species observed in the three systems studied. A wide variety of compounds has been investigated, and computer simulations have been performed to aid in the identification of the radicals which yielded complex spectra. A proposed mechanism for these reactions shall be presented and some observations as to the possible generality of this phenomena shall be offered.

M-PM-B13 ADAPTATION TO ETHANOL-INDUCED FLUIDIZATION OF BRAIN LIPID BILAYERS. David Johnson, Nancy Lee* and Roger Cooke, Univ. of Calif., San Francisco, CA 94143.

We show that ethanol is less able to fluidize reconstituted membranes formed from lipid extracts of tolerant mice synaptosomal membranes than those formed from controls. The effects of ethanol on membrane fluidity are assessed by fluorescence polarization technique. Acute in vivo administration of ethanol does not alter ethanol-induced fluidization of the bilayers. Bilayers formed from lipid extracts of membranes from pentobarbital tolerant mice show partial cross-tolerance with ethanol. These results suggest that changes in the lipid composition of membranes can account, at least in part, for tissue adaptation to anesthetic-induced membrane fluidization. Since increased membrane cholesterol has been suggested to account for ethanol tolerance, we equalized the level of cholesterol in both tolerant and control lipid extracts and measured the effect of ethanol. Even when the cholesterol level is equalized in the bilayers, it is still possible to measure differences between tolerant and control lipid extracts. This suggests that changes in membrane cholesterol do not account for tolerance.

M-PM-B14 REDUCED LATERAL MOBILITY OF A FLUORESCENT LIPID PROBE IN CHOLESTEROL-DEPLETED ERYTHROCYTE MEMBRANE. Nancy L. Thompson,* and Daniel Axelrod, Biophysics Research Division and Dept. of Physics, University of Michigan, Ann Arbor, MI. 48109

We have measured the effect of cholesterol depletion on the lateral mobility of a fluorescent lipid probe in the human erythrocyte plasma membrane. At low temperature (0° to 4°), the mobility of the probe was considerably more restricted in the cholesterol-depleted membrane than in non-depleted membrane. At high temperature (40°), probe mobility was not much affected by cholesterol depletion.

Whole erythrocytes were depleted of 30 - 50% of their cholesterol (as verified by biochemical assay) by 24h incubation at 37° with a sonicated dispersion of dipalmitoyl phosphatidylcholine. Cells were then labeled with 3,3'-dioctadecylindocarbocyanine (diI), a phospholipid-like fluorescent dye, and hemolyzed into spherical ghosts by hypotonic buffer. Ghosts were drawn into a capillary microslide and mounted on a temperature controlled microscope stage. The rate of lateral motion of diI was then quantitatively measured by signal averaging the fluorescence recovery after local photobleaching with a focused laser spot.

At 40°, diI mobility rates were approximately equal for both cholesterol-depleted and non-depleted ghosts. But at 0° to 4°, diI lateral mobility in depleted ghosts was reduced an average of eightfold from its 40° value, whereas in non-depleted ghosts the corresponding reduction from the 40° value was only about twofold. At low temperature, the mobility results on depleted ghosts were quite variable. Concomitant with this variability was the appearance of an inhomogeneous patchy distribution of diI fluorescence. Data variability and fluorescence patchiness were much less pronounced on non-depleted ghosts.

These results suggest that cholesterol suppresses aspects of phospholipid phase changes in animal cells in a manner consistent with its behavior in artificial bilayers and multilayers.

M-PM-C1 ON THE INCORPORATION OF GRAMICIDIN A CHANNELS INTO LIPID. Alberto Spisni*, Lanfranco Masotti*, M. A. Khaled* and Dan W. Urry, Laboratory of Molecular Biophysics, University of Alabama Medical Center, Birmingham, Alabama 35294.

Circular dichroism (CD) and carbon-13 (CMR) and sodium-23 magnetic resonance spectroscopies were utilized to assess incorporation of gramicidin A (GA) into lysolecithin micelles and lecithin liposomes. Criteria for incorporation were a CD pattern which was independent of the manner of gramicidin A addition, a CMR spectrum which demonstrated immobilization of the lipid interior, and sodium-23 spin lattice relaxation times which provided evidence of ^{23}Na interaction only when the preceding criteria were met. The CD spectrum obtained after heating for several hours at 60-70°C (or immediately on GA addition in trifluoroethanol) was characterized by a positive 220 nm band and negative CD below 205 nm. Heating caused the interior carbon-13 resonances of the lipid, the $-\underline{CH_2}-$ and $-\underline{CH_3}$ resonances, to broaden dramatically whereas the choline methyl resonances remained intense and sharp. The relaxation time of ^{23}Na, which was ~50 msec with water, with lipid in water, and with lipid in water plus GA before heating, decreased to 18 msec after heating appropriately to bring about the CD and CMR effects. Thus a lipid incorporated state of GA is defined and this state is required before interaction with an ion that can occupy the channel.

M-PM-C2 PARTITIONING OF CATIONS INTO THE GRAMICIDIN CHANNEL DETERMINED FROM CATION BLOCKAGE OF WATER FLUX. J.A. Dani* and D.G. Levitt, Department of Physiology, University of Minnesota, Minneapolis, MN 55455.

The channels formed by gramicidin in lipid bilayer membranes should be too narrow to allow water and cations to get around each other. If transport through the channels takes place by this single-file mechanism, then a cation in the channel should block water flux through that channel under open circuit conditions. Thus, it should be possible to determine the partitioning of cations into the channels from measurements of the water permeability of these channels as a function of cation concentration. Since the water flow through the channels must be large compared to the intrinsic water permeability of the lipid, it is necessary to use membranes that contain a large number of channels. A new procedure was used to incorporate gramicidin into the bilayer because standard techniques did not sufficiently increase the water permeability. Glycerol monoolein (1.5%)-hexadecane bilayers are formed at room temperature. After the bilayer is formed, it is cooled until the hexadecane in the torus freezes (about 17°C). Gramicidin dissolved in methanol is then pipetted directly at the bilayer. The membrane is then warmed to room temperature and the water flux produced by an osmotic pressure difference is measured. In the absence of ions this method reproducibly results in membranes with water permeabilities 30 times greater than that of undoped bilayers. The water flux alters the solute concentration in the unstirred layers next to the membrane. The effects of this solute polarization are corrected for by use of the membrane potential. Preliminary results indicate that the water permeability of the gramicidin containing bilayer is reduced about 15% in 0.1 M KCl and more than 90% in 1.0 M KCl.

M-PM-C3 SODIUM CHANNELS IN AXONS AND GLIAL CELLS OF MUDPUPPY OPTIC NERVE. G.R. Strichartz, C.M. Tang*, and R.K. Orkand*, Physiology and Biophysics, SUNY, Stony Brook, N.Y. 11794 and Physiology and Pharmacology, Dental Medicine, University of Pennsylvania, Philadelphia, PA 19104.

In 1976 Villegas et al[1] reported electrophysiological evidence for sodium channels in the Schwann cells of the giant axon of the squid, Sepioteuthis sepiodea. Here we report experiments to detect sodium channels in glial cells of the optic nerve of the mudpuppy, Necturus maculosa. Both binding experiments, using radiolabelled saxitoxin (*STX), and electrophysiological experiments using the sucrose-gap technique were conducted. Glial cells were studied in optic "nerves" from animals which had been enucleated 2 months before; such tissues lack axons. Saturable *STX binding was measured in optic nerves from normal animals; 2.2 ± 0.8 f-moles/mm length = total uptake at 5-20 nM *STX (14 samples); 0.35 ± 0.74 f-moles/mm length = uptake in presence of 10μM cold TTX(10 samples). No significant saturable *STX binding was detected in the all-glial tissue: 0.82 ± 0.59 f-moles/mm without TTX (11) versus 0.82 ± 0.87 f-moles/mm with TTX (8). Action potentials in normal optic nerves were reduced 50% in amplitude by ca. 7 nM STX. Veratridine and batrachotoxin produced a Na-dependent, TTX-sensitive depolarization of the normal optic nerve (27 mV by 10^{-6} M veratridine). Glial cells were only depolarized by [veratridine] $\geq 5 \times 10^{-4}$ M; the depolarization is irreversible and is not inhibited by STX. In summary, there is no evidence for sodium channels in Necturus glial cells when axons are absent.

[1] J. Gen. Physiol. 67, 369 (1976). Supported by USPHS NS12828 and NS 12253

M-PM-C4 SODIUM CURRENT OF SINGLE CARDIAC MUSCLE CELLS. K. S. Lee, R. Kao, T. Weeks, N. Akaike and A. M. Brown. University of Texas Medical Branch, Galveston, Texas 77550.

Heart muscle is a syncytium with restricted extracellular compartments. As a result spatial control of voltage and temporal resolution of fast kinetics are inadequate. We overcame this problem by dispersing individual heart muscle cells following the approach of Powell and Twist (BBRC, 1976) and Mehdi and Sachs (Biophys. J., 1978). Single myocytes are then sucked into a suction pipette utilizing a technique which allows voltage clamp and internal perfusion (Lee, Akaike and Brown, J. Gen. Physiol., 1978). After rinsing adult rat heart free of blood cells a buffer containing 0.1% collagenase (Sigma Type 1) and 0.1% hyaluronidase (Sigma Type 1) with 15mM glucose and the following salts (mM): NaCl 120.2; KCl 2.7; KH_2PO_4 1.4; $MgSO_4$ 1.4; CaCl 0.02; $NaHCO_3$ 13.6, equilibrated with 95% O_2 and 5% CO_2 was used for dispersion. Dispersed cells were harvested by spinning down at 24g and washed with enzyme-free buffer before suspension in Krebs-Henseleit solution. Myocytes break off at intercalated discs and heal over. Resting potentials are low but approach -90mV when isethionate$^-$ is substituted for Cl^-. I_K is suppressed by internal and external Cs^+ and I_{Ca} by Co^{2+} and/or zero Ca^{2+}. In 50% Na_o I_{Na}'s have no notches and show voltage dependent activation and inactivation. In lower $[Na]_o$'s I_{Na} is reduced without changes in kinetics or voltage dependence. I_{Na} is blocked by large doses of TTX and blockage is incomplete at positive potentials.

Supported by N.I.H. Grants HL-16657 and NS-11453.

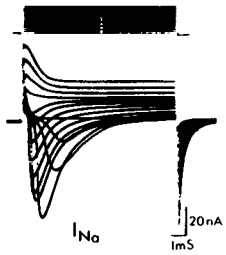

M-PM-C5 GATING KINETICS OF SINGLE ACETYLCHOLINE ACTIVATED CHANNELS MEASURED DURING "BURSTS" OF ACTIVITY FOLLOWING DESENSITIZATION. J. Patlak, B. Sakmann*, and E. Neher*. Max Planck Institut für biophysikalische Chemie, Göttingen, W. Germany.

The currents passing through single Acetylcholine (ACh) activated membrane channels can be recorded with an ACh containing patch electrode (1). At ACh concentrations above 5 μM, desensitization of the measured receptors eliminates most responses within 30 seconds. Subsequent recording yields only background noise and occasional "bursts" of activity. These bursts appear to be the activity of single channels which have returned from the desensitized state. It is improbable that bursts are caused by more than one channel because they have a low frequency of occurance (about one event in several minutes), and because the simultaneous openings of two or more channels are not observed during the burst. The open and closed intervals during a burst can be directly measured. The mean channel open time is approximately the same as in low concentration limit measurments, and is independent of concentration. The mean-closed-time is dependent on concentration, and is found to be equal to the mean-open-time when the agonist concentration is about 25 μM ACh. This agonist concentration compares well with the macroscopically measured apparent dissociation constant for ACh. The shape and slope of the mean-closed-time dose-response curve can provide information about the gating process of this channel.

J. Patlak is supported by a post-doctoral fellowship from the Muscular Distrophy Association of America.

(1). E. Neher, B. Sakmann, and J.H. Steinbach. Pflügers Arch., 375:219-228

M-PM-C6 IONIC SELECTIVITY OF END-PLATE CHANNELS. T.M. Dwyer, D.J. Adams* and B. Hille, Dept. Physiology and Biophysics, Univ. of Washington School of Medicine, Seattle, WA 98195.

Iontophoretic puffs of acetylcholine were applied to the frog neuromuscular junction under voltage clamp using the Hille-Campbell technique with the ends of a single muscle fiber cut in isotonic NaF. The reversal potential for end-plate current was determined when Na ions were replaced completely by 39 other cations. The solutions were buffered with 10 mM histidine and contained 1 mM $CaCl_2$. Permeability ratios P_S/P_{Na} were calculated from changes of reversal potential:

Cs	1.4	OH NH_3	2.0	OH guanidinium	1.7	ethyl NH_3	1.1
Rb	1.3	NH_4	1.8	guanidinium	1.6	dimethyl NH_2	0.9
K	1.1	NH_2 NH_3	1.3	NH_2 guanidinium	1.4	ethanol NH_3	0.7
Na	1.0	CH_3 NH_3	1.3	CH_3 guanidinium	0.8	diethyl NH_2	0.4
Li	0.9	$(CH_3)_3$ NH	0.4	$(NH_2)_3$ guanidinium	0.3	diethanol NH_2	0.3

Glucosamine, lysine and arginine cations have a relative permeability < 0.035. Diluting Na with glucosamine changed the reversal potential 21.3 mV per e-fold change in Na concentration, 86% of the expected value from the Nernst equation. Reversal potentials in mixtures of Na and K ions were those expected if P_K/P_{Na} has a constant value. Tris (0.2), choline and the divalent ions in the sequence Zn≈Ni≈Co≈Mg>Ca>Ba>Sr>Cd are all permeant. Triethanolammonium (0.09) is the largest permeant ion and requires a minimum channel opening of 6.5 x 6.5 Å. Tris and choline need an opening 5.5 x 5.6 Å and triaminoguanidinium, 3.5 x 6.6 Å. The end-plate channel is a large water-filled pore. (NIH grants NS 08174 and NS 05082, DJA is a Muscular Dystrophy Fellow.)

M-PM-C7 INTRACELLULAR K AND NA ON THE ANOMALOUS RECTIFICATION OF THE STARFISH EGG MEMBRANE. S. Hagiwara and M. Yoshii*, Department of Physiol., U.C.L.A., Los Angeles, CA 90024.

The effects of alterations of the intracellular ionic composition on the properties of anomalous or inward rectification of the egg membrane of the starfish, Mediaster aequalis, were studied by using an intracellular dialysis technique. The following results were obtained when the membrane current was analysed with voltage-clamp technique. (1) The inward rectification of the K conductance depends on $V-V_K$ when the K equilibrium potential, V_K is altered by changing $[K^+]_o$ at a fixed $[K^+]_i$. In contrast, it depends only on the membrane potential, V, when V_K is altered by changing $[K^+]_i$ at a fixed $[K^+]_o$. This leads to the conclusion that the gating of the K channel of the inward rectification depends on V and $[K^+]_o$, but not on $[K^+]_i$. (2) The conductance of the K channel at a given V is roughly proportional to the square root of $[K^+]_i$ when $[K^+]_i$ is altered at a fixed $[K^+]_o$. Since the conductance is proportional to the square root of $[K^+]_o$ when $[K^+]_o$ is altered at a fixed $[K^+]_i$, the final conclusion is that this conductance is proportional to the geometric mean of $[K^+]_o$ and $[K^+]_i$. (3) Intracellular Na^+ ions are necessary for the activation of inward rectification. A similar potentiating effect is found for Li^+, although it is weaker. Rb^+, Cs^+ and organic cations such as arginine$^+$ do not have this effect. Supported by NIH grant NS09012.

M-PM-C8 SINGLE GLUTAMATE ACTIVATED CHANNELS IN LOCUST MUSCLE. J. Patlak, K. Gration*, P. Usherwood*, and C. Patlak. Max Planck Institut für biophysikalische Chemie, Göttingen, W. Germany, and The University of Nottingham, Nottingham, England.

The currents which pass through single glutamate activated channels in the non-synaptic membrane of locust muscle have been measured. The single channel conductance is about 130 pS; the open-close transitions are much faster than the channel open time, thereby producing square pulses of current. A patch electrode similar to that used to measure single ACh channels in frog muscle (1) was used to electrically isolate a several micron diameter patch of membrane in the metathoracic extensor tibiae muscle of Locusta locusta. Adequate isolation could be obtained without enzymatic pre-treatment. Channels could occasionally be recorded in normal muscle fibers. However, in most experiments, one week denervation and a 15 minute pre-treatment with 1 μM Concanavalin-A were used to increase non-synaptic channel density and to remove desensitization, respectively. The current-voltage relation of these channels was linear between -40 and -130 mV, and had a slope of 133 pS. The zero current potential was -2 mV. The channel's most common mean-open-time was about 2 ms, but the gating kinetics were not stationary, and sudden changes in a single channel's mean open and closed times were observed.

J. Patlak is supported by a post-doctoral fellowship from the Muscular Distrophy Association of America.

(1). E. Neher, B. Sakmann, and J.H. Steinbach. Pflügers Arch., 375:219-228.

M-PM-C9 FLUCTUATIONS IN THE DARK CURRENT OF ROD PHOTORECEPTOR OUTER SEGMENTS. G. Matthews,* K.-W. Yau,* and D. A. Baylor. Stanford University, Stanford, California. 94305.

The current flowing across the membrane of single rod outer segments in pieces of isolated toad retina was recorded by drawing the outer segment into a close-fitting glass suction electrode connected to a current-to-voltage transducer. The steady inward current present in darkness was reduced by light. Spontaneous random fluctuations were observed in the dark current and consisted of two components: (a) occasional discrete events closely resembling the response to single absorbed photons, and (b) a smaller amplitude, continuous fluctuation apparently generated by superposition of shot effects occurring at relatively high frequency. The discrete events were present in complete darkness and may reflect thermal isomerization of rhodopsin molecules. The continuous component of current noise was found to arise from fluctuations in the membrane conductance of the outer segment. Power spectral analysis indicated that the shot effects underlying the continuous component were shaped by two of the four delay processes underlying the same cell's light response.

M-PM-C10 RATE THEORY MODEL OF THE Ca CHANNEL. S. Yasui*, A. M. Brown, N. Akaike and K. S. Lee. University of Texas Medical Branch, Galveston, Texas 77550.

Ca conductance in nerve is via channels and not carriers because the current noise power spectra are consistent with "channel" but not "carrier" noise (Akaike et al., Nature, 1978). Peak I_{Ca} saturates with small increases in $[Ca^{2+}]_o$ following a Michaelis-Menten relationship. This violates the Independence Principle and indicates that Ca ions interact with the channel. Eyring rate theory was applied to a simple two barrier, single site model of the channel following the approaches of Woodhull (J. Gen. Physiol., 1973) and Hille (Membranes, Vol. 3, 1975). A unique aspect is the increase in barrier heights as binding occurs. Experimental data were obtained from isolated neurons of Helix aspersa using the suction pipette method which combines voltage clamp with internal perfusion (Lee et al., J. Gen. Physiol., 1978). I_{Ca} was separated by suppression of I_{Na} and I_K's. The current sequence is $I_{Ba} > I_{Sr} > I_{Ca}$; Mg^{2+} and Be^{2+} are non-conducting. In the model, ion binding is responsible for saturation and the locations of the binding site or well and the two barriers felt by the permeating ions can be calculated using experimental data. These turned out to be similar for Ca, Ba and Sr with the well located about 0.6 of the "electrical" distance along the channel from its external mouth. The barriers are located at 0.15 and 0.95 of this distance. However, the energy levels for each ionic profile G_1^*, G_s^*, and G_2^* are different. The subscripts 1 and 2 refer to the external and internal barrier and the subscript s refers to the binding site. Relative values for Ca in units of kT are 14, -8.5 and 12 respectively. G_s^* is smaller for Sr and Ba and G_2^* is larger. Supported by N.I.H. Grants HL-16657 and NS-11453.

M-PM-C11 Ba CURRENT NOISE IN THE Ca CHANNEL OF NEURONS. N. Akaike, K. S. Lee and A. M. Brown (Intr. by D. L. Kunze). University of Texas Medical Branch, Galveston, Texas 77550.

Peak I_{Ba} is greater than peak I_{Ca} in neurons. Moreover I_{Ba} turns on faster and turns off slower than I_{Ca}. We measured Ba current noise in isolated Helix aspersa neurons using the suction pipette method and a low noise voltage clamp system (Akaike et al., Nature, 1978). I_{Na} and I_K's were suppressed beforehand. The recording bandwidth was 0.5 to 500 Hz and the spectra were computed with a Saicor spectral analyzer and/or digital computation using a fast Fourier transform program. Analysis was done on 15-30 sec blocks of data beginning some 10 sec after the voltage clamp step from a holding potential, V_H, of -60 mV. I_{Ba} was inactivating very slowly during this period. Control spectra were taken at V_H or after suppression of I_{Ba} with Co^{2+}. Ba noise spectra had simple Lorentzian shapes with a corner frequency, fc, of 7.1 ± 1.2 Hz (n = 8) and apparent unit conductance values, γ_{Ba}, of $6.7 \pm 1.1 \times 10^{-13}$ S. Under these experimental conditions, the fc for Ba is about half that for Ca and the unit conductances are about five times as great. The corner frequencies are similar to inactivation τ's from relaxation studies. The spectra were changed when voltages, $[Ba^{2+}]_o$'s and temperature were changed. Increased voltages and concentrations were associated with increased fc's and increased variances and decreased temperatures were associated with decreased fc's and decreased variances. Supported by N.I.H. Grants HL-16657 and NS-11453.

M-PM-C12 SODIUM CURRENTS IN NORMAL AND MYOTONIC MAMMALIAN SKELETAL MUSCLE FIBERS. T. E. DeCoursey* and S. H. Bryant (Intr. by R. J. Lipicky), Department of Pharmacology and Cell Biophysics, U. of Cincinnati College of Medicine, Cincinnati, Ohio 45267.

Sodium currents in skeletal muscle fibers from several mammalian species were examined at 12° C by the vaseline-gap voltage clamp technique of Hille and Campbell (J.Gen.Physiol. 67:265, 1976), with minor modifications. Data were obtained from external intercostal muscle fibers from 6 normal human volunteers, one patient with myotonic dystrophy, 13 normal goats, 14 goats with hereditary myotonia, and from sternomastoid muscles from normal rats and from rats (male Wistar) pretreated with a single large dose of 20,25-diazacholesterol (Dromgoole et al., Biochem.Med.13:307, 1975). Good control of the membrane potential was possible with goat and human fibers, while rat fibers were much smaller and therefore difficult to clamp. The precision of the measured parameters is limited by the existence of a prominent slow inactivation process with a time constant of several minutes around the holding potential.

Among the data to be presented are conventional current-voltage relationships, h-infinity vs. voltage curves, tau-h data obtained by varying pre-pulse duration, and kinetic data obtained by non-linear least squares fitting of individual current records to m^3h in the usual manner.

(This work supported by NIH Grant NS-03178 and an Albert J. Ryan Fellowship (T.E.D.).)

M-PM-C13 A COMPLETELY SYMMETRICAL BARRIER MODEL FOR ENDPLATE CHANNELS. Paul R. Adams, Department of Physiology, University of Texas Medical Branch, Galveston, Texas 77550.

Work with local anesthetics shows that the endplate channel contains a binding site for blocking cations about half way along its length, flanked by 2 barriers. Decamethonium (DECA) can also bind to this site and hop the distal barrier. Perhaps the energy profile seen by blockers - a proximal barrier, a midchannel well and a distal barrier - is also experienced by Na and K. Na and K are roughly equally permeant in endplate channels, and have equal total inside and outside concentrations. In symmetrical solutions the I-V relation will only show the observed symmetry when the two barriers are equal. Under these conditions, the model predicts a single channel current that varies as sinh (eV/4kT). This function is almost linear in the range $\pm$ 100 mV, in agreement with the linearity of the normal endplate I-V relation. It predicts linear increase in $\underline{i}$ and $\exp(eE_{rev}/kT)$ with external Na, if the well is far from saturation. Recalculation of Lewis' data (J. Physiol., in press) shows that both these conditions are met, provided the external K level was twice that in the Ringer, due to leakage from fibers, and provided the rate constant k_x for the outside $\rightarrow$ well transition is about 1.4 greater for potassium than for sodium. The effects Lewis sees with Ca are consistent with the model if the Ca affinity is about 25 mM and the k_x about 0.2 that of Na. However the main test of the model is provided by Case et al's (J. Physiol. 272: 295) demonstration of equal inward Na and DECA fluxes. If the potential in these experiments was -80 mV, this implies that k_x for Na is 2.8 that for DECA. Using the observed DECA blocking rate constant (2×10^7 $M^{-1}s^{-1}$), this gives $k_{Na} = 5 \times 10^7$. Now the model predicts a single channel conductance $e^2xk_xk_{-x}/2kT(k_{-x} + x.k_x)$ where x is the ion concentration and k_{-x} the rate constant for leaving the channel. Since for sodium $k_{-x} >> k_x x$, the combined DECA blocking and flux data give a γ of 16 pS, close to the true value.

M-PM-D1 REGULATION OF THE CONTRACTILITY OF CARDIAC CONTRACTILE PROTEINS. G. McClellan and S. Winegrad, Dept. of Physiology, Univ. of Penn., School of Medicine, Phila., Pa. 19104.

The properties of the contractile proteins of rat heart have been studied in small bundles of cardiac cells from the right ventricle which were made hyperpermeable to ions and small molecules by treatment with EGTA. In these hyperpermeable fibers, adding epinephine, c-AMP, c-GMP or GTP to either the relaxing or contracting solution had no obvious effect on contractility unless a low concentration of detergent was present during the exposure to the drug. When added with a detergent, these drugs affected the contractility in a consistent way. Epinephrine and c-AMP produced an increase in contractility. Cyclic GMP and GTP enhanced the contractility as well but the increase was closely related to the existing catecholamine stimulation. Cyclic-GMP also had an inhibitory effect on the contractility that could be separated from the stimulatory effect. From the kinetics of the two responses to cGMP it appears that the stimulatory and inhibitory effects probably involve respectively the membrane and the cell interior. These observations can be explained by a regulatory system in which the β receptors are coupled to adenylate cyclase in the membrane by guanine nucleotides and result in the activation of a membrane bound protein kinase. A phosphorylation of the contractile proteins by the catalytic subunit from this protein kinase is probably responsible for modifying the contractility as measured with direct application of Ca^{++}. This reaction is different from the one involved in the regulation of Ca sensitivity (McClellan and Winegrad, J.G.P. Nov. 1978) and indicates that a different protein kinase is probably involved. (Supported by USPHS grant HL16010).

M-PM-D2 REGULATION OF SMOOTH MUSCLE MYOSIN LIGHT CHAIN KINASE BY THE CATALYTIC SUBUNIT OF ADENOSINE 3':5'-MONOPHOSPHATE DEPENDENT PROTEIN KINASE. M.A. Conti, D.R. Hathaway*, C.B. Klee*, R.S. Adelstein, NIH Bethesda, Maryland 20014.

Turkey gizzard smooth muscle myosin light chain kinase (MW 125,000±5,000) purified by CDR-Sepharose affinity chromatography (CDR = calcium dependent regulatory protein, MW 16,500) gives a single protein band by polyacrylamide gel electrophoresis under denaturing and non-denaturing conditions. The specific activity of the kinase is approximately 15 μmol P_i transferred/mg/min at 24° using the isolated 20,000 dalton light chain of smooth muscle myosin as substrate. The smooth muscle myosin light chain kinase is phosphorylated by the catalytic subunit of beef heart cAMP-dependent protein kinase. One mole of phosphate can be incorporated per mole of myosin light chain kinase at 1/3 the rate found when histone IIA is used as substrate for the protein kinase. Incorporation of phosphate into the myosin light chain kinase is inhibited by 80% in the presence of the protein kinase inhibitor. Limited tryptic digestion (4 min, 0°, 250:1 mg: mg ratio myosin light chain kinase: trypsin) cleaves the enzyme into a single, radioactive peptide (MW 22,000) and an 80,000-100,000 dalton polypeptide. Both the phosphorylated and the unphosphorylated forms of the enzyme require Ca^{++} and CDR for activity. Phosphorylation of smooth muscle myosin light chain kinase results in a decreased affinity of this enzyme for CDR and therefore a decreased rate of phosphorylation of smooth muscle myosin light chains when subsaturating levels of CDR are present.

M-PM-D3 X-RAY SCATTERING OF MYOSIN LIGHT CHAINS IN SOLUTION. J.E. Hartt and R.A. Mendelson, Cardiovascular Res. Inst., U.C.S.F., San Francisco, CA 94143

Skeletal muscle myosin is believed to be composed of two heavy chains (HC) and four light chains (LC) in a stoichiometry 1HC : 1 LC-2 : 1 LC-1 or LC-3. Our group has previously reported X-ray scattering data from subfragment-1 (Kretzschmar, Mendelson, & Morales (1978). Biochem. 17, 482). In conjunction with these studies and since the functions of the light chains localized on S1 are currently under investigation by many methods, we have examined their general shape and size isolated in solution (50 mM Tris, 50 mM KCl, pH 7.8, no added Ca^{++}, concentration range 10-40 mg/ml). Our specimens included the three types of LC's from rabbit back muscle and the regulatory LC-2 from scallop myosin (kindly supplied by Prof. A.G. Szent-Gyorgyi). It has been found that both LC-2's are elongate objects with radius of gyration and axial ratio of presumed anhydrous prolate ellipsoids of revolution (assumed partial specific volume 0.73 cc/gm) of 23±1.5 A and 4.9 for rabbit and 21.8±0.5 A for scallop. The alkali LC is more spherical, giving 18.5±1 A and 3.5 for LC-3. These data agree well with hydrodynamic measurements of Stafford and Szent-Gyorgyi ((1978), Biochem. 17, 607) and Alexis and Gratzer ((1978) Biochem. 17, 2319). A preliminary measurement on LC-1, however, indicated it to be somewhat shorter than LC-2, in disagreement with Alexis and Gratzer.

This work was supported by NIH Grants HL-06285, HL-16683, HL-07192-02 and NSF Grants PCM 75-22698, PCM 76-11491, and NSF DMR 73-07692 in cooperation with Stanford Linear Accelerator Center and Dept. of Energy.

M-PM-D4 HYBRID FORMATION USING SCALLOP MYOFIBRILS AND REGULATORY LIGHT-CHAINS FROM OTHER SPECIES. P. D. Chantler*, J. R. Sellers* and A. G. Szent-Györgyi (Intro. by L. Makowski) from Department of Biology, Brandeis University, Waltham, Massachusetts 02154.

Scallop myofibrils, treated with 10mM EDTA at 25-30° to remove all regulatory light-chains, do not bind calcium and there is no calcium-dependent enhancement of the actin-activated Mg^{++}-ATPase (Chantler, P. D. and Szent-Györgyi, A. G. (1978). Biophys. J. 21. 45a). This is in contrast to a similar treatment at 0° which only removes one regulatory light-chain per myosin molecule. The 30°-desensitized preparation facilitates formation of pure hybrids obtained by the readdition of light-chains from other species. Only one class of light-chain is rebound to the scallop myosin heavy-chain (this class is defined as regulatory for it restores calcium sensitivity to 0°-desensitized scallop myofibrils). Light-chain uptake can be monitored by gel electrophoresis on 15% SDS or urea gels. The pure hybrids thus formed fall into two groups. One group of hybrids restores calcium binding and calcium sensitivity to 30°-desensitized scallop myofibrils; these hybrids were formed with the regulatory light-chains from various molluscan muscles or chicken gizzard and cricket leg muscles. The other group of hybrids are formed using regulatory light-chains from rabbit skeletal, bovine cardiac and lobster tail muscles; this class neither restores calcium-binding nor calcium sensitivity to 30°-desensitized scallop myofibrils. The results obtained with hybrids using rabbit skeletal, bovine cardiac and chicken gizzard regulatory light-chains were independent of the phosphorylation state of those light chains.

This work was supported by a British-American Heart Association Fellowship to P.D.C. and by Public Health Service (AM-15963) and the Muscular Dystrophy Association (78-0214 CE) grants to A.G.S.G.

M-PM-D5 EFFECTS OF ANTI-SCALLOP MYOSIN LIGHT CHAIN ANTIBODIES ON MYOSIN LINKED REGULATION. Theo Wallimann*and Andrew G. Szent-Györgyi, Dept.Biology, Brandeis Univ.Waltham, Mass. 02154.

Antibodies obtained against regulatory (R-LC) and "essential" (SH-LC) of scallop myosin were specific and did not cross-react with the heterologous LC in immuno-diffusion, -electrophoresis,-replica tests and radioimmunassays. Both anti-R-LC IgG and anti-SH-LC IgG abolished the calcium dependence of the actin activated Mg-ATPase of scallop myofibrils at ratios of 2.5 - 3 moles of IgG bound per mole of myosin by elevating the Mg-ATPase activity in the absence of Ca. The Mg-ATPase activity in the presence of Ca and the K/EDTA ATPase activity were reduced to about one half by the anti-SH-LC IgG. Neither of these antibodies had an effect on the high-Ca-ATPase (10mM Ca) or on Ca-binding. Anti-R-LC IgG prevented the extraction of R-LC by EDTA. Binding of anti-R-LC IgG to myofibrils was proportional to their R-LC content. Increased amounts of anti-SH-LC IgG were bound by myofibrils devoid of R-LC. The bound anti-SH-LC antibody significantly inhibited the re-uptake of R-LC. Monovalent anti-R-LC Fab' fragments desensitized myofibrils fully and induced a significant (70%) dissociation of R-LC with a concomitant reduction of Ca-binding. Anti-SH-LC Fab' also desensitized myofibrils to a full extent but, in contrast to the anti-SH-LC IgG, no longer inhibited the Mg-ATPase in the presence of Ca. Anti-SH-LC Fab' did not dissociate any LC or reduce the Ca-binding. Certain rabbits produced a population of anti-SH-LC antibodies which was specific for the SH-LC and strongly bound to myofibrils but failed to desensitize them. The results confirm the regulatory function of the scallop R-LC and strongly suggest a direct or indirect involvement of the SH-LC in myosin linked regulation with a possible interaction between the R-LC and the SH-LC.

Supported by fellowships from the Swiss NSF and Muscular Dystrophy Assoc. (MDA) to T. W. and by PHS-(AM 15963) and MDA grants to A.G.S.G.

M-PM-D6 ELECTROPHORETIC STUDY OF A RELATIONSHIP BETWEEN MYOSIN LIGHT CHAINS 1 AND 2. T. Hozumi*, K. Ue*, and J. Botts (Intr. by J. Duke), CVRI, UCSF, San Francisco, Ca 94143

Vertebrate fast skeletal myosin is isozymic, containing light chain LC_1 or LC_3. DTNB-treatment of myosin is known to remove only about half of light chain LC_2 from myosin, suggesting that it may be removed from one isozyme and not the other. We prepared subfragment-1 (S-1) from DTNB-treated myosin using Mg^{++}-papain in order to minimize damage to the remaining LC_2. This S-1 was applied to a DEAE-cellulose column (the same method used for separation of S-1 isozymes in chymotryptic preparations). Although the separation was in complete, the ascending portion of the peak was largely S-1(LC_1, LC_2) whereas the descending portion was largely S-1(LC_3). Thus, the loss of LC_2 during DTNB-treatment is mainly from the S-1(LC_2, LC_3) isozyme. Secondly, we observed the interaction between LC_2 and chymotryptically prepared S-1 isozymes, using polyacrylamide gel electrophoresis of the native proteins. Addition of LC_2 speeded up the migration of S-1(LC_1), but the mobility of S-1(LC_3) was essentially unchanged, suggesting that LC_2 has a stronger affinity for the former and forms with it the complex S-1(LC_1, LC_2). Our results show that LC_2 is difficult to remove from S-1(LC_1, LC_2) but easy to remove from S-1(LC_2, LC_3) and, conversely, that LC_2 interacts strongly with S-1(LC_1) but may have little affinity for S-1(LC_3). This research was supported by NHLBI, NSF, and AHA; T.H. is a Fellow of the AHA.

M-PM-D7 PROTEOLYTIC DIGESTION OF GIZZARD MYOSIN AND THE REGULATION OF ACTIN-ACTIVATED ATPase. John C. Seidel, Dept. of Muscle Res., Boston Biomed. Res. Inst., Boston, MA.

Limited digestion of chicken gizzard myosin with α-chymotrypsin (CT) produces a heavy meromyosin, HMM-1, that can be phosphorylated by a partially purified light chain kinase and has actin-activated ATPase activity only in the presence of Ca^{2+} and regulatory proteins, a preparation containing light chain kinase and tropomyosin. The apparent molecular weight of this fragment is 310,000, based on gel filtration on Sepharose 4B and subunit molecular weights from gel electrophoresis in SDS. More extensive digestion with CT leads to HMM-2, a fragment that has greatly reduced Ca^{2+}-dependent phosphorylation and actin-activated ATPase, but little loss of Ca^{2+} or K^{+} ATPase without actin. Under non-denaturing conditions, HMM-1 and HMM-2 show the same migration on polyacrylamide gel electrophoresis and the same elution volume on gel filtration. These values fall between those of HMM and S-1 from rabbit skeletal muscle. Subsequent digestion of either HMM-1 or HMM-2 with papain (P) produces a fragment whose ATPase activity is activated fully by actin in the absence of regulatory proteins and Ca^{2+}. A similar fragment, S-1(P), is produced by direct digestion of gizzard myosin with papain. Subsequent digestion of S-1(P) with CT leads to loss of all ATPase activity. These fragments exhibit one of three patterns of ATPase activity in the presence of actin: i) a fully regulated activity (HMM-1), ii) a depressed activity (HMM-2), which is converted to iii) an unregulated activity [S-1(P)] on digestion with papain. The results can be most easily explained in terms of a myosin-linked regulatory mechanism, the regulatory site, i.e. the site of phosphorylation, and the actin binding site being in different regions of the myosin molecule. Supported by grants from NHLBI (HL-15391) and MDA.

M-PM-D8 PHOSPHORYLATION OF MYOSIN LIGHT CHAIN ON STIMULATION OF INTACT SMOOTH MUSCLE. S.P. Driska & R.A. Murphy, Dept. Physiology, U. Va. Med. Sch., Charlottesville, VA 22908.

Activation of smooth muscle actomyosin MgATPase by Ca^{2+} is dependent on phosphorylation of the 20,000 dalton light chain of myosin (LC20). We have attempted to determine if this phosphorylation occurs on contraction of intact living smooth muscle strips whose mechanical performance could be measured. Phosphorylation of LC20 was estimated by the shift of its isoelectric point (pI) when homogenates of muscle strips or purified myosin were analyzed by two dimensional isoelectric focusing/SDS electrophoresis (IEF/SDS). LC20 could be resolved into 3 components with pI's ≈ 5.70, 5.57, and 5.48. When actomyosin was incubated with $MgAT^{32}P$, the ratio of components changed from 0.82:0:0.18 (basic:middle:acidic) in the presence of EGTA, to 0.23:0.52:0.25 in the presence of Ca^{2+}. Autoradiography of the IEF/SDS gels showed most of the ^{32}P was present in the middle component. To test for changes of light chain phosphorylation on contraction, 4 pairs of pig carotid artery media strips were prepared. The maximum active force for the tissues at their optimum lengths was $2.72 \pm 0.53 \times 10^5$ N/m^2 (±SD). One tissue of each pair was stimulated isometrically with K^{+} and frozen at peak force by immersion in -78°C acetone. The other tissue of each pair was frozen without stimulation. The frozen tissues were homogenized and analyzed by IEF/SDS. On stimulation of the muscle strips, (1) the basic component decreased significantly, from 70.2 ± 4.6% to 51.7 ± 4.5% (±SEM, N=4); (2) the middle component increased significantly, from 4.2 ± 4.2% to 32.0 ± 1.7%; and (3), the acidic component showed no significant change (25.6 ± 6.4% to 16.3 ± 2.1%). While these results show that phosphorylation of LC20 occurs on contraction of intact living smooth muscle, the estimated changes in phosphorylation of LC20 were less than those observed in actomyosin preparations. Supported by NIH grants PO1 HL19242, P60 AM22125, and F32 HL05180.

M-PM-D9 RADIOLABELING OF THE LC_{20} MYOSIN LIGHT CHAIN OF SKINNED SMOOTH MUSCLE EXPOSED TO ATP^{32} OR $ATP\gamma S^{35}$. P.S. Cassidy, P.E. Hoar, W.G.L. Kerrick, Dept. of Physiology & Biophysics, Univ. of Wash., Seattle, WA 98195.

Two different types of vertebrate smooth muscle were studied to determine the relationship between phosphorylation of the LC_{20} myosin light chain in skinned muscle preparations and the active tension development. Rabbit ileum strips, skinned with staphylococcal α-toxin or Triton X-100, incorporated a maximum of 0.004 moles P^{32} per mole LC_{20} under low calcium conditions and 0.050 under maximally activating high calcium conditions. These values were not significantly increased by the presence of a nucleotide regenerating system or by stopping the phosphorylation reaction by different methods. Chicken gizzard, skinned mechanically, incorporated 0.01 and 0.20 moles P^{32} per mole LC_{20} respectively under low and high calcium conditions. The incorporation of P^{32} was completely reversed by returning to low calcium conditions in both types of muscle. Very different results were obtained when the muscle preparations were exposed to $ATP\gamma S^{35}$. Skinned rabbit ileum incorporated 0.04, 0.75 and 0.69 moles $S^{35}P$ per mole LC_{20} under low calcium, high calcium, and a return to low calcium conditions respectively, and chicken gizzard incorporated 0.1, 0.8 and 0.5 moles $S^{35}P$ under the same conditions. The reversible labeling of the LC_{20} myosin light chain with ATP^{32} as the nucleotide and the irreversible labeling with $ATP\gamma S^{35}$ as the nucleotide correlate well with our previous finding that incubation in ATPγS induces an irreversible activation of tension in skinned smooth muscle preparations. Despite the difference in the maximum incorporation of P^{32} and $S^{35}P$, the maximum tensions which could be attained were not significantly different. The significance of these data in relation to light chain kinase activation of smooth muscle will be discussed. (Supported by PHS HL 07090, Muscular Dystrophy Assn., and American Heart Assn.)

M-PM-D10 ISOLATION OF FUNCTIONAL CARDIAC MYOFIBRILS AND MYOSIN LIGHT CHAINS WITH IN VIVO LEVELS OF LIGHT CHAIN PHOSPHORYLATION. R. J. Solaro, M. J. Holroyde*, D. Small* & E. Howe*, University of Cincinnati, College of Medicine, Cincinnati, OH 45267.

A simple and reproducible technique for the determination of the levels of myosin light phosphorylation in heart muscle has been developed in order to probe relations between alterations in light chain phosphorylation and biochemical and mechanical cardiac function. Conditions were developed in which we could prepare functional myofibrils from freeze-clamped beating hearts with the state of myofibrillar myosin light chain phosphorylation chemically "frozen" during the extraction procedure. Phosphorylation of light chains was inhibited maximally with 5 mM EDTA. Dephosphorylation of light chains was maximally inhibited with 70 mM NaF and 50 mM KH_2PO_4-KOH, pH 7.0. We prepared the myofibrils by a modification of the procedure of Solaro et al. (Biochim. Biophys. Acta, 245:259-262,1971) using an inhibiting buffer containing 50 mM KH_2PO_4-KOH, pH 7.0, 70 mM NaF, 5 mM EDTA. Myofibrils were shown to be functionally intact by measurement of calcium binding and ATPase activity. No significant change in the state of myosin light chain phosphorylation was observed during myofibrillar preparation as judged by processing cardiac myosin labeled with ^{32}P and ^{125}I together with myofibrils through the procedure. Highly purified cardiac light chain fractions could be routinely isolated from myofibrillar preparations using an ethanol fractionation step together with DEAE-cellulose chromatography. Levels of light chain phosphorylation were determined by analysis of the phosphate and nitrogen content of the whole light chain fraction together with determination of the proportion of P-light chain in the fraction by SDS polyacrylamide gel electrophoresis. (Supported by AHA grant 74-865 NIH grants HL 22231 and HL 22619 , R.J.S. was supported by Research Career Development Award HL 000464.)

M-PM-D11 EFFECT OF PHOSPHORYLATION OF MYOSIN LIGHT CHAIN IN INTACT FROG MUSCLE ON THE BOUND CALCIUM OF ACTIN. M. Bárány and K. Bárány, University of Illinois Medical Center, Chicago, 60612

Recently, we have shown phosphorylation-dephosphorylation of the 18,000-dalton light chain of myosin during the contraction-relaxation cycle of frog muscle (K. Bárány, M. Bárány, J.M. Gillis and M.J. Kushmerick, Biophys. J. 21, 44a, 1978). However, no turnover of the light chain-bound phosphate was found during ATP hydrolysis catalyzed by the Mg^{2+} and Ca^{2+}-activated myofibrillar ATPase. This suggests a special role for light chain phosphorylation in the muscle. We postulated that the phosphoryl group attached to the myosin head could form a bond with the actin-bound calcium and thereby increase the affinity of cross-bridge attachment to the thin filament. The actin-bound calcium was labeled in live muscle by injecting ^{45}Ca into frogs. Light chain was maximally phosphorylated in the dissected muscles by caffeine-treatment (K. Bárány and M. Bárány, JBCh. 252, 4752, 1977), the untreated contralateral muscles served as controls, containing the light chain in partially phosphorylated form. Myofibrils were prepared from both treated and untreated muscles in the presence of a strong Ca-chelating agent, and their Ca-content was determined both by radioactive and analytical methods. The myofibrils from the caffeine treated muscles contained about 1 mole Ca per mole actin, and the fibrils from untreated muscle contained less than a half mole Ca. The ratio of light chain phosphorylation (caffeine/control) in these myofibrils was similar to the ratio of the Ca-content of their actins, indicating that the phosphoryl group on the light chain protected the actin-bound calcium against removal by the Ca-chelating agent. (Supported by NS-12172 from NIH and MDA).

M-PM-D12 PHOSPHORYLATION AND TENSION GENERATION IN FUNCTIONALLY SKINNED STRIATED MUSCLE FIBERS. P.E. Hoar, P.S. Cassidy, W.G.L. Kerrick, Dept. of Physiology and Biophysics, University of Washington, Seattle, WA 98195.

Ca^{2+}-activated tension generation and protein phosphorylation were measured in functionally skinned muscle fibers (sarcolemma disrupted) under similar conditions. We observed no correlation between phosphorylation of myosin light chains and tension generation in rabbit cardiac and skeletal (slow-twitch soleus) skinned fibers. In order to eliminate possible effects of any remaining sarcolemma membrane, as well as the sarcoplasmic reticulum, soleus and cardiac fibers were treated with a 1% solution of the detergent Triton X-100. This treatment was found to have no significant effect on the Ca^{2+}-activated tension of either muscle type, although it caused a general decrease in the phosphorylation level of all proteins of the soleus fibers including myosin light chain-2. It is known that ATPγS is a substrate for both skeletal and smooth muscle myosin light chain kinase, and that thiophosphorylated proteins are resistant to phosphatases. We have previously shown that irreversible labeling of the 20,000 dalton light chain by $ATP\gamma S^{35}$ is responsible for active tension generation of smooth muscle in the presence of ATP and the absence of Ca^{2+}. Nevertheless, thiophosphorylation of the myosin light chain-2 of soleus or cardiac skinned fibers was not observed under the same conditions used for smooth muscle. Although phosphorylation may play a role in the modulation of tension in the intact system, it does not appear to affect the Ca^{2+} sensitivity of skinned striated muscle fibers.
(Supported by the Muscular Dystrophy Association, the American Heart Association, and U.S. Public Health Service grant HL 07090.)

M-PM-E1 ELECTRICAL AND ION SELECTIVE PROPERTIES OF RHODOPSIN CONTAINING MEMBRANES. David S. Cafiso and Wayne L. Hubbell, Department of Chemistry, University of California, Berkeley, CA 94720

A series of spin labeled probes have been synthesized which respond to transmembrane potentials or pH gradients in small vesicles. The use of these phosphonium and secondary amine spin labels (which can be used to quantitate $\Delta\psi$ and ΔpH, respectively) has revealed two interesting features of rod outer segment discs and rhodopsin-phospholipid recombinant membranes: 1) Reconstituted vesicles containing purified bovine rhodopsin have a high K^+ ion selectivity in the dark giving rise to large transmembrane potentials in the presence of ion gradients; this selectivity is modulated by light; 2) A fast photovoltage has been detected in native bovine disc membranes and appears to be associated with a potential change in the boundary region of the membrane. The uptake of a proton at the external interface by rhodopsin may be responsible for this change.

Supported by NIH Grant EY 00729

M-PM-E2 EFFECT OF DITHIOTHREITOL ON THE LIGHT-INDUCED PERMEABILITY OF RHODOPSIN-PHOSPHOLIPID MEMBRANE VESICLES. **D. F. O'Brien, R. A. Ott,* and P. N. Tyminski,* Eastman Kodak Company, Research Laboratories, Rochester, N.Y. 14650.**

Rhodopsin-phospholipid membrane vesicles were prepared from purified bovine rhodopsin and phospholipids by detergent dialysis. These thermally stable and light-sensitive membranes were loaded with Ca^{2+} or other divalent cations by sonication followed by gel permeation chromatography. Unexposed membrane vesicles entrap the divalent cations, which may be photoreleased by flash exposure with green light. The photorelease of Ca^{2+} was determined with the dye Arsenazo III. Membrane vesicles prepared from rhodopsin in detergent in the absence of dithiothreitol (DTT) show large photoreleases of Ca^{2+} (40 to 160 Ca^{2+}/rhodopsin bleached) at low levels of rhodopsin bleaching. Membrane vesicles prepared in the presence of mM DTT show only limited photorelease of Ca^{2+}. This effect of DTT on the photorelease of Ca^{2+} is observed only when DTT is present prior to the detergent dialysis formation of the membrane vesicles. The significance of these observations will be discussed with regard to the sulfhydryl content of rhodopsin and the functionality of rhodopsin in membranes.

M-PM-E3 DETERMINATION OF THE TRANSVERSE LOCATION OF RETINAL IN ROD OUTER SEGMENT DISC MEMBRANES: FLUORESCENCE ENERGY TRANSFER IN THE RAPID-DIFFUSION LIMIT. David D. Thomas, William F. Carlsen*, and Lubert Stryer, Department of Structural Biology, Sherman Fairchild Center, Stanford University School of Medicine, Stanford, CA 94305.

Fluorescence energy transfer can be enhanced by translational diffusion of donors relative to acceptors. The rapid-diffusion limit corresponds to $D\,\tau_o/s^2 \gg 1$, where D is the sum of the diffusion coefficients of the donor and acceptor, τ_o is the donor lifetime in the absence of transfer, and s is the mean distance between donors and acceptors. In the rapid-diffusion limit, the energy transfer rate is proportional to a^{-3}, where a is the distance of closest approach between donors and acceptors (Thomas, Carlsen, and Stryer, PNAS, December, 1978). We have achieved the rapid-diffusion limit by using Tb^{3+} chelated to dipicolinate as a long-lived energy donor (τ_o = 2.1 msec). This technique can be used to measure the distance a from the aqueous surface of a protein or membrane to a chromophore buried within it. For rhodopsin solubilized (monomeric) in the detergent ammonyx LO, the distance of closest approach between the centers of chelated Tb^{3+} and retinal (the acceptor chromophore) is 20 Å, indicating that retinal is deeply buried within the protein. Chelated Tb^{3+} was trapped inside rhodopsin-containing vesicles by sonicating rod outer segment disc membranes in a solution of chelated Tb^{3+}. External Tb^{3+} was removed by Sephadex chromatography, and subsequent Tb^{3+} leakage was negligible during the course of the experiments. The vesicles retained the sidedness of native disc membranes. Energy transfer experiments were performed on this preparation and on vesicles having only external Tb^{3+}. The results indicate that retinal is closer to the inside surface of the disc membrane than to the outside surface.

Supported by research grants from the National Institutes of Health.

M-PM-E4 THE RESONANCE RAMAN SPECTRUM OF THE L INTERMEDIATE IN BACTERIORHODOPSIN. D.L. Narva and R.H. Callender, Physics Dept., City College of New York, N.Y., 10031. Resonance Raman spectra of photostationary state mixtures of bR568, L, and M for light adapted bacteriorhodopsin were obtained at several temperatures between -20C and -80C. The relative concentrations of the different pigments in the photostationary mixture were varied by both temperature and also by simultaneous sample irradiation with a "pump" laser beam. The Raman spectrum of L was obtained by computer subtraction techniques using the known Raman spectra of bR568 and M. A major band in this spectrum at 1652 cm^{-1} strongly suggests that the L intermediate of the bacteriorhodopsin photocycle contains a retinal-opsin protonated Schiff base linkage, a result which is contrary to earlier reports. Thus, the chromophore of bacteriorhodopsin would appear to deprotonate in the L to M transformation. Deuterium experiments are in progress to prove whether the Schiff base of L is protonated. There are differences in the spectrum of L relative to bR568 in the fingerprint region, suggesting that some chromophore conformational change has occurred.

M-PM-E5 THE RESONANCE RAMAN SPECTRUM OF BATHORHODOPSIN: IMPLICATIONS FOR MODELS OF VISUAL EXCITATION. B. Aton*, A. Doukas*, D. Narva, R.H. Callender, Physics Dept., City College of New York, N.Y., N.Y. 10031, and B. Honig, Dept. of Biological Sciences, Columbia University, New York, N.Y. 10027.

Resonance Raman spectra at 77°K of photostationary state mixtures of rhodopsin, bathorhodopsin and isorhodopsin were obtained. The compositions of the mixtures were determined and the bathorhodopsin spectrum was isolated by computer subtraction techniques. The C=N stretching frequency of the Schiff base is found to be nearly identical in all three pigments. This shows that there is no change in the state of protonation of the Schiff base nitrogen as a result of the rhodopsin-bathorhodopsin transformation. This precludes a number of recent models for the primary event. The spectral features of bathorhodopsin in the fingerprint region are significantly different than those of rhodopsin, indicating that a conformational change in the chromophore has taken place. The bathorhodopsin spectrum is also different than that of model all-trans protonated Schiff bases in solution although here, some similarities are evident. Given the large body of evidence supporting a cis-trans isomerization for the primary photochemical event, the Raman data suggest that the chromophore of bathorhodopsin is strained trans ("transoid") rather than pure all-trans. Our recent model for the primary event shows that "strain" is a natural consequence of isomerization in the protein. The essence of the model (see Honig et al; these proceedings) is that isomerization cleaves a salt bridge leading to charge separation and, thus, to a high energy state.

M-PM-E6 RESONANCE RAMAN STUDIES OF BATHORHODOPSIN: EVIDENCE FOR A PROTONATED SCHIFF BASE LINKAGE.* G. Eyring* and R. Mathies, Chemistry Dept., Univ. of Calif., Berkeley, CA 94720.

We have used a dual beam, coaxial pump-probe laser technique (Oseroff and Callender, Biochemistry, 13, 4243 (1974)) to optimally enhance the Raman scattering from bathorhodopsin in a photostationary steady state mixture of pigments formed at -160°C. Spectra of pure rhodopsin and isorhodopsin, weighted by their measured concentrations and relative Raman cross sections, have been subtracted to yield a Raman spectrum of pure bathorhodopsin. Bathorhodopsin has lines at 853, 875, 920, 1006, 1166, 1210, 1278, 1323, 1437 and 1536 cm^{-1}. In addition, batho displays a protonated Schiff base vibration at 1657 cm^{-1} which shifts upon deuteration to 1625 cm^{-1}. Since the protonated Schiff base lines of rhodopsin and isorhodopsin have nearly identical frequencies and deuterium shifts, it is clear that neither the $C=NH^+$ nor the $N-H^+$ bond order is changed when bathorhodopsin is formed. Recently, a number of structures have been proposed for bathorhodopsin that involve proton translocation. Our results on the Schiff base vibration contradict the predictions of several of these models. In further experiments using an intensified vidicon detector together with pulsed laser excitation, the Raman scattering of a photostationary steady state mixture of rhodopsin, isorhodopsin, and bathorhodopsin has been observed at room temperature. Under these conditions the three characteristic lines of bathorhodopsin are found at 858, 873, and 920 cm^{-1}. The fact that the frequencies of these lines are nearly identical at both temperatures implies that the retinal conformation in bathorhodopsin formed at room temperature is the same as that formed at -160°C.

*This work was supported in part by NIH grant EY-02051.

M-PM-E7 LIGHT-DARK ADAPTATION IN TRITON-SOLUBILIZED PURPLE MEMBRANE
Rita Casadio, H. Gutowitz, P. C. Mowery, R. H. Lozier and W. Stoeckenius, Department of Biochemistry and Biophysics, Cardiovascular Research Institute, University of California, San Francisco, California 94143

Exposure to light reversibly shifts the absorption maximum of purple membrane from 558 to 568 nm and causes an increase in optical density of 14%. Extraction of dark-adapted membrane yields equal amounts of 13-cis and all-trans retinal, light-adapted membrane yields only all-trans retinal. Solubilization in Triton X-100 for two days at room temperature and in the dark shifts the absorption maximum to 548 nm and decreases the optical density by 12%. Exposure to light now causes a reversible red-shift of 4 nm and optical density absorbance increase of 2%. Extraction of dark-adapted solubilized purple membrane yields a 60:40 13-cis:all-trans isomer ratio and light adaptation changes the isomer ratio to 40:60. The light-dark difference spectra of intact and solubilized purple membrane are nearly identical, suggesting that a fraction of the solubilized membrane preparation behaves like intact membrane in agreement with the change in the ratio of isomers. However, ultracentrifugation (1) and CD spectra show only bacteriorhodopsin monomers to be present. All experiments were carried out at pH 5.0 in 0.1 acetate buffer and at 25° C. (Supported by NIH GM23651-02, HL06285-18, NSF PCM-7611801, NASA NSG-07151.)

(1) Reynolds, J. A. and Stoeckenius, W. Proc. Natl. Acad. Sci. USA 7 2803 (1977)

M-PM-E8 TIME-RESOLVED RESONANCE RAMAN STUDIES OF THE INTERMEDIATES OF BACTERIORHODOPSIN.
J. Terner, C. L. Hsieh,* A. R. Burns,* and M. A. El-Sayed, University of California, Los Angeles, California 90024.

We are studying the intermediates of bacteriorhodopsin by resonance Raman spectroscopy in an attempt to obtain more detailed information about the mechanism of the photo-induced proton pumping cycle, than is obtainable from transient optical absorptions. We have most recently obtained the resonance Raman spectra of the bL_{550} and bO_{640} intermediates in the region from 800 to 1800 cm^{-1}. Additionally the spectrum of light adapted bR_{570} has been subtracted from dark adapted bR^{DA}_{560} to obtain the spectrum of the 13-cis(?) form. Comparison of the spectra obtained by suspending purple membrane in H_2O and D_2O has yielded information about the state of protonation of the Schiff base linkage in the particular intermediates. Examination of the fingerprint region (1100 - 1400 cm^{-1}) has revealed information about changes in the conformation of the retinal chromophore during the photosynthetic cycle as well as the dark adaptation process.

M-PM-E9 COMPARATIVE STUDIES ON THE RELATIVE QUANTUM YIELD AND TRANSIENT PROTONATION CHANGES OF PURPLE MEMBRANE SUSPENDED IN VARIOUS MEDIA.
R.H. Lozier, H. Niv*, S.-B. Hwang, P. Havel*, R.A. Bogomolni and W. Stoeckenius. Cardiovascular Research Institute, and Department of Biochemistry and Biophysics, University of California, San Francisco, CA 94143.

In contrast to the difference in values reported in the literature (1-4) the quantum yield of the photocycle in light-adapted purple membrane suspensions in H_2O, 0.2M KCl and basal salt/ether were found to be the same within ±6% (the amplitude of the flash-induced transient absorbance change was followed at 410 nm, pH 7.0, 25°C).

Proton release and uptake has been measured by pH indicator dyes (7-hydroxycoumarin and p-nitrophenol) at pH 7.0 and 7.8 at 25 and 45°C. The results confirm an increase in proton release with increasing ionic strength as measured by other techniques (5,6). The only proton release step is observed after the "M" intermediate has been formed; proton uptake brings the pH to the initial value with the formation of "O" and/or bR. This result is inconsistent with the 3-step proton release/uptake scheme $\ldots \xrightarrow{-H^+} M \xrightarrow{+2H^+} O \xrightarrow{-H^+} bR$ suggested by Fischer and Oesterhelt (7).

1. Oesterhelt, D. and Hess, B., Eur. J. Biochem. 37,316-326 (1973).
2. Lozier, R.H. and Niederberger, W., Fed. Proc. 36, 1805-1809 (1977).
3. Goldschmidt, C.R., Kalisky, O., Rosenfeld, T. and Ottolenghi, M., Biophys. J. 17, 179-183 (1977).
4. Becher, B. and Ebrey, T.G., Biophys. J. 185-189 (1977).
5. Hess, B., Biophys. Struct. Mechanism 3, 68 (1977).
6. Ort,D. and Parson, W.W., personal communication.
7. Fischer, U. and Oesterhelt, D., poster session at the EMBO workshop, Juelich, Oct. 1976, and personal communication.

M-PM-E10 PHOTOSENSORY BEHAVIOR OF MOTILE HALOBACTERIUM HALOBIUM. J.L. Spudich*and W. Stoeckenius. Cardiovascular Research Institute, and Department of Biochemistry and Biophysics, University of California, San Francisco, CA 94143.

Temporal changes in light intensity modulate swimming behavior in H. halobium (1). The flagellar responses to light are mediated by two photoreceptors, one of which (the PS565 receptor) is bacteriorhodopsin (2). The second receptor (the PS370 receptor) has not yet been identified, but function of the PS370 photosensory system is known to be suppressed by growth in the retinal synthesis inhibitor, nicotine, and restored by retinal addition (3).

By using selection procedures based on the chemotactic sensitivities of the cells, we have isolated a highly motile strain of H. halobium. With individual cell tracking methods we have found that both the suppression (by a temporal decrease in light intensity) and the enhancement (by a temporal increase in light intensity) of flagellar reversal mediated by PS370 are inhibited by nicotine growth and restored by retinal. Growth in nicotine does not alter the spontaneous reversal frequency of the cells nor inhibit their chemotactic response. Since the retinal requirement appears to be specific to the photosensory responses, these data support the suggestion that the PS370 receptor is a retinylidene protein, perhaps a precursor of bacteriorhodopsin (3).

By imposing patterns of light and chemical gradients on soft (0.3%) agar plates, we can separate cells lacking the photosensory responses from normally responsive bacteria. These methods are being applied to the selection of bacteriorhodopsin and PS370 receptor mutants.

1. Oesterhelt, D. and Stoeckenius, W. Proc. Natl. Acad. Sci. U.S.A. 70, 2853-2857 (1973).
2. Hildebrand, E. and Dencher, N. Nature 257, 46-48 (1975).
3. Hildebrand, E. Biophy. Struct. Mechanism 3, 69-77 (1977).

M-PM-E11 SECONDARY PROTEIN CHROMOPHORE INTERACTIONS IN BACTERIORHODOPSIN. Ann T. Lemley*, Aaron Lewis and Henry Crespi†, (Intr. by R. E. Cookingham), School of Applied and Engineering Physics, Cornell University, Ithaca, N. Y., 14853, and Chemistry Division Argonne National Laboratories, Argonne, Illinois, 60435.†

Resonance Raman spectra of naturally occurring and isotopically labelled purple membranes indicate that a secondary protein Schiff base interaction is present in bacteriorhodopsin (bR_{570}) which is apparently absent in the M_{412} intermediate. This conclusion is the result of a systematic investigation of C=N and $C{=}\overset{H}{N}$ + vibrational modes in membranes containing fully protonated and deuterated retinal in fully protonated or fully deuterated opsin, membranes fully enriched with ^{15}N, and various model Schiff bases of retinal. In addition, to establish the specific nature of the interaction, we studied in H_2O and D_2O fully deuterated purple membranes selectively labelled with protonated amino acids. These selectively labelled systems contained either protonated lysine, protonated tyrosine, protonated arginine or protonated tryptophan. Analyses of the constitution of these systems will be discussed, and the Raman spectra will be reviewed.

M-PM-E12 THE EXCHANGE RATE OF DEUTERONS BY PROTONS AT THE SCHIFF BASE IN BACTERIORHODOPSIN, B. Ehrenberg and A. Lewis (Intr. by R. K. Clayton), Cornell University, Ithaca, N. Y., 14853.

Kinetic resonance Raman spectroscopy has been used to measure the exchange rate of deuterons by protons at the Schiff base in bacteriorhodopsin. Our experiments were performed on suspensions of purple membrane fragments in D_2O which were mixed rapidly with H_2O in a mixer having a dead time of 1·5 msecs. To measure the exchange time we monitored the appearance of the C = N ⊕ H stretching frequency at 1642 cm^{-1} and the disappearance of the C = N ⊕ D stretching frequency at 1620 cm^{-1}. It was found that the exchange at pH 7 proceeds with a rate constant of 0·17 $msec^{-1}$. The exceptionally slow rate of exchange is an indication that the properties of this proton are significantly altered from those observed for an unperturbed, readily accessible Schiff base. Other experimental data suggest[1] that the Schiff base proton is interacting with an amino acid residue (probably lysine) in the bacterio-opsin matrix. Our results on the exchange time are certainly consistent with this suggestion.

1 A. Lewis, M. A. Marcus, B. Ehrenberg and H. Crespi, Experimental evidence for secondary protein-chromophore interactions at the Schiff base linkage in bacteriorhodopsin: Molecular mechanism for proton pumping, Proc. Natl. Acad. Sci. (USA) 75, 4462-4466 (1978).

M-PM-E13 VIBRATIONAL SPECTRA OF PURPLE MEMBRANES WITH NANOSECOND RESOLUTION: RESONANCE COHERENT ANTI-STOKES RAMAN SCATTERING (CARS) OF BACTERIORHODOPSIN, Edward T. Nelson*, Aaron Lewis and Ross A. McFarlane* (Intr. by G. P. Hess), School of Applied and Engineering Physics, Cornell University, Ithaca, N. Y., 14853.

To probe the vibrational spectra of bacteriorhodopsin (bR_{570}) and K at room temperature resonance coherent anti-Stokes Raman spectra of purple membranes have been obtained using short pulse (6·5 ns) excitation at a pump wavelength of 580 nm where the line shape was Lorentzian. Unlike cytochrome c a pronounced saturation of the raman line intensity with associated broadening of lines was observed for laser intensities resulting in an absorption of more than 100 photons/molecule per pulse. This broadening is consistent with a transient heating of the sample. Under these conditions of high laser intensity no bleaching of the sample was observed, ruling out excited state and lifetime broadenings. At laser intensities where no broadening of the vibrational features could be detected, the CARS spectra (within the range of 1450-1675 cm^{-1}) were identical with the spectra of bacteriorhodopsin (bR_{570}) obtained using CW excitation. At K/bR = 0·29 no spectral features were found that could be attributed to K.

M-PM-E14 COULD THE EMISSION OF BACTERIORHODOPSIN (bR_{570}) RESULT FROM A DIPOLE-ALLOWED TRANSITION?, Aaron Lewis, School of Applied and Engineering Physics, Cornell University, Ithaca, N. Y., 14853.

It has generally been assumed that bacteriorhodopsin (bR_{570}) emission results from a dipole forbidden transition.[1,2,3] This is reasoned mainly from analogy with polyene emission spectra. A crucial element in this analogy is the emission quantum yield (ϕ_F) which yields, together with the measured emission lifetime, radiative lifetimes which are 8 to 20 times longer than the intrinsic lifetime of 7 nsec calculated by the Strickler-Berg relationship. However, ϕ_F has been calculated in these systems assuming that every photon absorbed does indeed populate the emitting state. This may not be a good assumption for bacteriorhodopsin. We reason this from two observations: (1) The temperature dependence of the emission lifetime[4] and K production kinetics[5] show that the emission and photochemistry proceed along different paths. (2) The observation that the photochemical quantum yields for the forward (bR→K) and reverse (K→bR) reactions sum to one[6] indicates that most of the molecules proceed along the path of photochemistry. Therefore, it is quite possible that ≥90% of the molecules never reach the emitting minimum and thus cannot be considered in calculating ϕ_F. This suggests that the fluorescence quantum yields at room and low temperature are probably ≥90% higher than those reported previously and this significant upward adjustment of ϕ_F could give radiative lifetimes of ≤9 nsec, in agreement with calculations based on the Strickler-Berg relationship. In view of these results we have to conclude that bacteriorhodopsin (bR_{570}) emission could result from a dipole-allowed transition.

[1] Lewis et al., Nature 260, 675 (1976). [2] Alfano et al., Biophys. J. 16, 541 (1976). [3] Hirsch et al., Biophys. J. 16, 1399 (1976). [4] Shapiro et al., Biophys. J. 23, 383 (1978). [5] Kaufmann et al., Biophys. J. 22, 121(1978). [6] Goldschmidt et al., Biophys. J. 17, 179 (1977).

M-PM-F1 THE ROLE OF INTRACELLULAR CALCIUM IN THE AUTOMATICITY OF EMBRYONIC HEART CELL AGGREGATES. W.T. Clusin Stanford University School of Medicine, Stanford, Ca., 94306

Several experiments indicate that diastolic depolarization in beating chick embryonic heart cell aggregates results from a decline in potassium permeability that is mediated by removal of ionized calcium from the sarcoplasm. Membrane resistance increases during diastolic depolarization and the maximum diastolic potential varies with extracellular K. Diastolic depolarization is accelerated following brief intracellular injections of EGTA. Longer injections cause a sustained but temporary depolarization to about -25 mV. External application of cobalt or a low calcium saline (Ca:EGTA of 1:2) produces a similar reversible depolarization. Further depolarization by current pulses does not produce hyperpolarizing after-potentials. Changes in intracellular ionized calcium during diastolic depolarization can be inferred by optical monitoring of edge movements with a photodiode. These measurements show that diastolic depolarization is accompanied by progressive relaxation, which continues until the next beat. This relaxation is due to a continued reduction in intracellular ionized calcium because it is accelerated by premature termination of the action potential plateau, or by intracellular injection of EGTA. Changes in automaticity that result from cooling, spontaneous variation or overdrive suppression are all accompanied by changes in the rate of relaxation: faster relaxation accompanies faster diastolic depolarization. There is a fixed relation between diastolic membrane potential and edge position which is not altered when automaticity is modified by the factors listed above. These data indicate that changes in beat frequency that result from cooling, spontaneous variation and overdrive suppression are due to changes in the rate at which intracellular free calcium is removed. (Supported by a grant from the California Heart Association.)

M-PM-F2 ANALYSIS OF THE VOLTAGE DEPENDENCE OF GAP JUNCTION CONDUCTANCE IN AMPHIBIAN EMBRYOS - A. L. Harris*, D. C. Spray, M. V. L. Bennett, A. Einstein Coll. Med., NYC 10461

Junctional conductance (g_j) between Ambystoma blastomeres in isolated pairs is voltage dependent. Steady state g_j decreases as a steep function of transjunctional voltages of either polarity though there is a small voltage insensitive conductance. In order to measure g_j directly, a double voltage clamp technique was devised. Each cell of a coupled pair was placed in a separate voltage clamp circuit and held at its resting potential. One cell was given voltage steps and junctional current (I_j) measured as the current supplied by the clamp on the other cell to keep its membrane potential constant. Decline of g_j during a transjunctional voltage step and the recovery of g_j following termination of the voltage step both occur in a simple exponential manner. This suggests a simple two state model for the conductance elements, where the governing rate constants are voltage sensitive. The voltage sensitive component of g_j in the steady state can be well fit by an expression of the form $g_j = \frac{g_{max}}{1+\exp -A(V-V_0)}$ where $A = nq/kT$. The ratio $g/(g_m-g)$ changes e-fold for about a 4mV change in transjunctional voltage for small voltages ($n=6 \cdot 3$). When the polarity of transjunctional voltage steps is reversed, the junctional conductance shows transient recovery, suggesting that conductance elements open before closing when the electric field across them is reversed, as if there were independent and symmetrical gates.

M-PM-F3 CYCLIC AMP INCREASES JUNCTIONAL PERMEABILITY IN CULTURED MAMMALIAN CELLS. J. Flagg-Newton* (Intr. by W.R. Loewenstein), Department of Physiology & Biophysics, Univ. of Miami School of Medicine, Miami, Fl. 33101.

Exposure of 3T3 Balb/C and B fibroblasts (sparse cultures) to cyclic AMP (1mM) or dibutyryl cyclic AMP (1mM) produces increase of junctional permeability; the proportion of test junctions transmitting the fluorescent peptide probes LRB Glu_2 or LRB Glu_3 increases. In Balb-C cells, permeability improvement progresses over a period of 4h, declines to base level within the next 2h, and falls below that level within 24h. In B cells, the permeability stays near peak for at least 24h. A condition of equivalence to the permeability declining phase may exist during prolonged confluency where intracellular cyclic AMP level in Balb/C cells is known to be elevated; permeability here is subnormal. No such major junction effects were seen in LRB liver epithelioid cells.

M-PM-F4 INTRACELLULAR pH CONTROLS CONDUCTANCE OF EMBRYONIC GAP JUNCTIONS - D.C. Spray, A.L. Harris*, M.V.L. Bennett, A. Einstein Coll. Med., NYC 10461
Agents expected to lower intracellular pH decrease electrotonic coupling in crayfish septate axon and between pairs of blastomeres from cleavage stages of Ambystoma or Fundulus embryos. Equilibration of the bathing saline with 100% CO_2 (pH 5.8) quickly and reversibly uncouples cells in each of these tissues. Treatment with membrane permeant anions (acetate, propionate) that should acidify the cytoplasm also cause a reversible decrease in coupling, and this effect is potentiated by lowering pH of the saline. Voltage clamp analysis and measurement of input and transfer resistances under current clamp show that pH uncoupling is associated with decreased junctional conductance of typically 2 to 3 orders of magnitude while non-junctional conductance remains constant. Membrane impermeant strong acids are without profound effect. Pressure injection of concentrated solutions of MOPS buffer (pH 7.4) into one cell of a coupled pair reduces or slows the effect of uncoupling treatments. The slight voltage sensitivity of Fundulus gap junctions and the steep voltage dependence of junctional conductance in blastomeres of Ambystoma are eliminated or greatly reduced during recovery of electrotonic coupling following CO_2 uncoupling. This effect of low pH on voltage dependence may indicate a common locus of action on the intercellular molecule mediating junctional conductance. Supported by NIH grants HD 02428, NS 12627, NB07512. DCS is a McKnight Scholar in Neuroscience.

M-PM-F5 CHARACTERIZATION OF GIANT MOTOR SYNAPSES OF DIFFERENT MORPHOLOGIES IN THE CRAYFISH CNS. J. Margiotta* and B. Walcott. SUNY at Stony Brook, Stony Brook, New York 11794.

Furshpan and Potter (J. Physiol, 1959) determined that transmission at giant motor synapse (GMS) from lateral giant interneuron (L.G.) to giant flexor motoneuron (F_1) is electrical, and that the synaptic membrane rectifies, the impedance being lower for orthodromic (L.G. to F_1) than for antidromic currents. Our experiments reveal striking differences in the morphology of these segmental synapses. In the last thoracic ganglion (T_8), the L.G. and F_1 are apposed for over 800 µm. In the second abdominal ganglion (A_2), the contact area extends for only 250 µm. We are comparing the physiological properties of the GMS at T_8 and A_2 in order to determine whether this difference in contact size plays any role in determining the functional properties of identified electrical synapses. Microelectrodes placed in L.G. and F_1 are used to apply current pulses to one cell while the membrane potential of both cells is recorded. Current is then applied to both cells and adjusted to make the potential in each cell the same. This procedure makes the difference in potential across the synapse (V_s) zero. The current-voltage (IV) characteristics of the functionally isolated cells may then be determined, and an IV curve for the synapse constructed. Curves thus obtained from GMS at T_8 and A_2 reveal differences in transmission. Consistent with its morphology, the T_8 GMS, having a larger contact area, typically has a lower impedance to antidromic currents (R_s= $1.08\times10^6\Omega$, 6 expts.) than does the A_2 GMS (R_s=$5.45\times10^6\Omega$, 3 expts.). Synapses at both locations show decreased impedance to orthodromic currents beyond a positive V_s. Surprisingly, however, the impedance decreases to a similar value (R_s=$0.100-.110\times10^6\Omega$, 9 expts.), although this occurs at a higher V_s in the case of the A_2 GMS. We believe mechanisms other than a difference in contact area must account for the latter findings.

Supported by USPHS AM 18750.

M-PM-F6 MICROSCOPIC AND MACROSCOPIC DESCRIPTIONS OF A SYNCYTIUM. V. Barcilon, RS Eisenberg, and R.T. Mathias, Dept. of Physiology, Rush University, Chicago, IL 60612.

Interpretation of the electrical properties of a syncytial tissue, or a cell invaginated with tubules, requires a theory to relate measurements of induced voltage or current flow to the properties of the structures which comprise the tissue. Such a theory has previously been derived using a physically motivated macroscopic approach. We now derive macroscopic equations from the exact equations for the microscopic electric field in the intracellular and extracellular media of the syncytium. A limited set of realistic assumptions are made, namely the membranes within the tissue are taken to be good electrical insulators compared to salt solutions and the diameter of the tubules is taken to be much smaller than the diameter of the preparation. These assumptions imply that the tubules can be approximated as noninteracting one dimensional electrical cables. Partial differential equations similar to those previously reported (Biophys. J., Jan. 1979) are derived to describe the potentials U_i & U_e in the intracellular and extracellular media. The boundary condition previously used is not recovered; rather, it is replaced by

$$\frac{1}{R_i}\frac{\partial U_i}{\partial n} = -Y_s U_i + \frac{\chi}{R_e}\frac{\partial U_e}{\partial n}$$

where R_i & R_e are the effective intracellular and extracellular resistivities, defined as the product of the true resistivities and a combination of morphometric parameters, Y_s is the admittance of the surface membrane (mho/cm^2), n is the outward normal, and χ is a parameter determined by the angular distribution, tortuosity, and volume fraction of the tubules close to the surface membrane of the preparation.

M-PM-F7 HOW REGIONAL INHOMOGENEITIES AFFECT CARDIAC ACTION POTENTIAL PROPAGATION. R. Joyner and G. Sharp, Univ. of Iowa, Iowa City, Iowa 52240.

Numerical simulations of propagation of action potentials in cardiac tissue strands have been done using the Crank-Nicholson implicit integration method to solve cable equations in which the membrane properties for each cable segment are represented by a cardiac membrane model (either Beeler and Reuter, 1975, or McAllister et. al., 1976) for ventricular muscle or Purkinje fibers, respectively. The ability to specify any parameter of the membrane model as a function of distance along the strand allowed us to investigate the effects of regional changes in membrane properties. In particular, we have shown that abrupt changes in the membrane properties produce widespread changes in the shape of the propagated action potential. We produced regional delayed repolarization by changing the membrane model in certain regions to produce a five fold change in the duration of the repolarization phase but did not observe rebound excitation. Regions of lowered excitability ($\bar{g}Na=0$) produced block unless the regions were also depolarized, in which case the "slow response" was initiated. The model presented may prove useful in establishing a physical basis for propagational phenomena in cardiac tissue. Supported by NIH grant HL22562 to Dr. Joyner.

M-PM-F8 VOLTAGE CLAMP STUDIES OF ELECTROTONIC COUPLING IN PERFUSED CRAYFISH SEPTATE AXONS. M. Johnston* and F. Ramón, Dept. Physiol., Duke Univ. Med. Ctr., Durham, N.C. 27710.

Septate (lateral giant) axons from the abdominal nerve cord of the crayfish are about 100 μm in diameter and superficial on the ventral surface of the cord. Individual segments (5-10 mm long) are coupled at each ganglion by electrotonic synapses located in the septum between the axon segments. To study the mechanism by which these synapses effect coupling, we have developed two techniques: (a) internal perfusion of the segmented axons, and (b) voltage clamp of the septum. Internal perfusion is achieved by inserting a cannula (50 μm in diameter) into the axon and advancing the tip close to the septum. Solutions flow out of the tip of the cannula and leave the axon by the cut where the cannula was introduced. For voltage clamp experiments two cannulas, one on either side of the septum, are used for current injection and measurement, and internal microelectrodes record the transseptal potential. Application of TTX, TEA, or other blocking agents minimizes the contributions of the external surface membrane to the measured currents. Our results show that the currents are symmetrical about zero potential for up to 10 msec, indicating a linear voltage dependence of the coupling mechanism. Supported by NIH Grants HL22767 and NS03437.

M-PM-F9 THE MECHANISM OF POLARITY CONTROL IN PLANARIANS AND EMBRYOS OF HIGHER ANIMALS: AN EXAMINATION OF SOME TESTABLE CONSTRAINTS IMPOSED BY THE BIOELECTRIC-ELECTROPHORETIC MODEL. C.S. Lange, University of Rochester, N.Y. 14642.

The problem of tissue polarity determination has long eluded an answer at the molecular level. Developing embryos and adult organisms of species with high regeneration capabilities have been classical systems for the study of this determination. The planarian has been the most extensively studied such species. Et. Wolff et scuola did much to elucidate the cellular basis of the planarian's extensive regenerative capabilities and underlined the central role of the brain in a series of inductions and inhibitions. Th. Lender et scuola showed that cell-free extracts of planarian heads could inhibit or prevent brain regeneration in decapitated planarians. They also found comparable activity in similar extracts of chick embryo heads assayed in planarian regenerates, indicating the likelihood of a common mechanism. Steele & Lange purified and characterized the protein responsible for this inhibition of differentiation to form brain tissue, and proposed a bioelectric-electrophoretic model to explain the mechanism of polarity control. This model made two a priori unexpected predictions - (1) that a caudad-positive cephalad-negative bioelectric field should exist and (2) remain intact postdecapitation - both of which were shown to be correct. Here we propose to examine further developments of the model and some further predictions and/or imposed constraints. This paper is based on work performed in the Department of Experimental Radiology under U.S.D.O.E. Contract No. EY-76-S-02-3501.

M-PM-F10 IONIC MECHANISMS UNDERLYING NEUROTROPHIC ACTION ON MEMBRANE RESTING POTENTIAL OF CULTURED CHICK SKELETAL MUSCLE. J.K. Engelhardt, K. Ishikawa*, W. J. Driskell*, and D.K. Katase*. Dept. of Neurology, USC School of Medicine, Los Angeles, CA. 90033.

Skeletal muscle resting potentials (V_m) decline following denervation. This is an interesting phenomenon in view of recent reports that neurotrophic factors act on membrane chloride conductance (G_{Cl}). If chloride ions are distributed passively, changes in G_{Cl} should not affect V_m. The experiments discussed here were designed to look for neurotrophic effects on the internal potassium ion concentration ($[K]_i$) or on the membrane permeability to potassium (P_K) that might explain the observed neurotrophic effect on V_m.

Resting potentials and component ionic conductances were determined in pure muscle cultures and in muscle co-cultured with spinal cord explants in bathing solutions of various ionic composition. These measurements indicated:

1) $[K]_i$ is not affected by neurotrophic factors.

2) P_K determined in 25 mM $[K]_o$ (so that $V_m=V_K$) was 20% larger in muscle that had been co-cultured with spinal cord explants.

3) Current-voltage (I-V) curves in low Cl^- solutions (presumably K-channel I-V relations) demonstrated inward going "anomalous" rectification. Physiological $[K]_o$ (2.7-5.4 mM) resulted in a V_m that was well positive to V_K which placed the K-channel in the low conductance region of its I-V relation.

Conclusion: While there appears to be a neurotrophic increase in P_K, the nonlinear I-V relation of the K-channel allows other ions (e.g., Cl^-) to make major contributions to the membrane electrical properties at physiological potassium ion concentrations.

(Supported by grants from The Amyotrophic Lateral Sclerosis Society of America (ALSSOA), The Myasthenia Gravis Foundation, The Wright Foundation, and NCI grant #CA22885).

M-PM-F11 SENSORY CONTROL OF PARAVERTEBRAL MUSCLE DIFFERENTIATION IN YOUNG AND ADULT DOGS. G. Maréchal, L. Plaghki" & W. Lokietek",U.C.L., 55 Av. Hippocrate, B-1200 Bruxelles (Belgium).

Five right posterior spinal roots (thoracic 5 to 10) were transected in the epidural space between the spinal ganglion and the medulla in 6 months old Beagle dogs (n = 4), taking great care not to damage the anterior roots. No paralysis was observed. A scoliosis consolidated in about 1 month, its curve being convex to the operated side (35° to 50°, Cobb's Method). Samples of five muscles were taken on each side at the apex of the scoliotic curve. Right ilio-costalis and intertransversalis had 1.5 to twice more AMPdeaminase, CPK, PFK, aldolase, pyruvate kinase, LDH and MDH (NAD), and 1/3 less ICDH (NAD-P) than controls (sham operated, n = 4), left muscles being similar to controls. Right trapezius and latissimus dorsi muscles were less modified, having 5 to 20 % more glycolytic enzymes, CPK and AMP deaminase, and 10 to 15 % less ICDH than the controls; the left muscles were similar to the controls. Right and left intercostalis had the same enzyme contents than the control. In adult dogs (n = 4) section of five posterior spinal roots produced a very slight scoliosis : the enzymic content of deep ilio-costal and superficial ilio-costal muscles remained the same than those found in sham operated adult dogs (n = 4).

Thus sensory informations modulate the enzymic differentiation of the homolateral homometameric muscles in growing dogs, but not in adult dogs. The strength of this influence is maximal for deep paravertebral muscles, is less for superficial dorsal muscles and is not observable for parietal muscles.

M-PM-F12 DERIVATION OF CELL LINES FROM THE CEREBELLUM G. J. Giotta and M. Cohn*, Salk Institute, San Diego, California 92112, P.O. Box 1809.

We have successfully isolated nerve and glia cell lines derived from the cerebellum of rats and mice after infection with Rous sarcoma virus which is temperature-sensitive for transformation. These lines express transformed or normal phenotypes when grown at the permissive (PT) or non-permissive temperature (NPT) of the virus respectively. For example, cells grown at the NPT and characterized as to plasma membrane proteins, growth in agar, morphology, growth rate, "contact inhibition" and lactate dehydrogenase isoenzyme profile, respond in a manner identical to normal non-transformed cerebellar cells. If, however, the cells are grown at the PT and subjected to similar analyses, all six criteria reveal the cells to be transformed. Presently these lines are being screened as to their neuronal or glial nature. The major criteria used to judge lines as neurons is the presence of voltage dependent sodium channels as revealed by 1) the influx of radioactive sodium in the presence of the sodium channel activator veratridine, and 2) electrical excitability. The former assay has revealed that approximately 30% of the clones contain voltage-dependent sodium channels and recent testing of one of these clones has shown it to be electrically excitable. The remaining clones have been classified as glia. Thus, this technique successfully yields both neuronal and glial cell lines from the cerebellum with apparent normal physiology.

Supported by Grant #1R23CA-24393-01 CBY, awarded by the National Cancer Institute, DHEW, to G. J. Giotta, and CA09254 to M. Cohn.

M-PM-F13 | PATTERNING IN GROWING CELL SHEETS: A MODEL FOR NEURAL RETINA. L. Bodenstein* and R.K. Hunt (Intr. by M. Larrabee), Thomas C. Jenkins Department of Biophysics, The Johns Hopkins University, Baltimore, MD 21218.

During development many cell sheets undergo intraspecific differentiation based on cell position and leading to the formation of complex patterns. As an example, the vertebrate neural retina undergoes position-dependent differentiation yielding a two-dimensional array of positional information which mediates the formation of a precise retino-tectal projection later in development. Evidence indicates that positional information in the retina is coded with reference to Cartesian axes. In contrast, the retina grows by cell accretion at the periphery, from a ring of stem cells, with polyclones extending outward from the center as spokes in a wheel: growth is best modeled as a radial phenomenon. We have developed a model to account for the deployment of Cartesian information along a radially growing sheet. The model states that each newly formed cell attempts to replicate the positional values of the cell immediately antecedent to it within the polyclone; the replication, however, is altered by a specific 'undershoot' or 'overshoot' operation. The precise nature of this operation is encoded in a system of operators which is maintained along the circumference of the retina (the ring of stem cells): only this system of operators is open to embryonic regulation. Information, although transmitted radially in accord with growth, is always coded in Cartesian variables. Simulations have shown the model can account for the normal state of the retina as well as results obtained after experimental perturbations. In addition, the model is capable of deploying a wide variety of coding systems across a wide variety of sheet geometries at the cost of a slight implicit redundancy.

Supported by NIH (NS-14807) and NSF (PCM-77-26987).

M-PM-G1 RETINAL LIGHT DAMAGE AS A FUNCTION OF WAVELENGTH. W. T. Ham, Jr., H. A. Mueller,* and J. J. Ruffolo, Jr., Virginia Commonwealth Univ., Richmond, VA 23298.

Exposure of limited areas of the retina of the rhesus monkey to visible and near infrared radiation produces lesions which are primarily thermal or photochemical in type depending on wavelength and duration of exposure. An action spectrum for minimal lesions has been determined for eight monochromatic laser lines extending from 1064 to 441 nm. Exposure to 1064 nm for 1000 s produces a typical burn lesion at elevated retinal temperatures (23°C) whereas a similar exposure to 441 nm produces a photochemical lesion at power levels too low to induce an appreciable temperature rise (<0.1°C). The two types of lesions differ in a number of respects as will be discussed. To further elucidate the differential effects on the retina of short vs long wavelength light we have exposed the retina to a series of nine wavebands between 400 and 735 nm, using sharp cut filters in conjunction with a 2500 W xenon lamp. The waveband 435-735 nm required a radiant exposure of 200 J/cm^2 to produce a minimal lesion whereas the waveband 675-735 nm required 1350 J/cm^2. The 200 J/cm^2 exposure produced predominantly photochemical damage whereas the 1350 J/cm^2 lesion was a retinal burn. The effect of wavelength on retinal light damage will be discussed in terms of solar retinitis and other photopathologies of the retina. (Joint support: U.S. Army Medical Research and Development Command, NIH-NEI Grant EY-02324-01, and Corning Glass Works.)

M-PM-G2 DNA INJECTION PROTEINS AS THE TARGET OF ACRIDINE SENSITIZED PHOTOINACTIVATION OF PHAGE P22. J. Bryant, Jr.*, and J. King, M.I.T., Cambridge, Mass. 02139

In an attempt to identify the target of the lethal damage, we have re-investigated acridine photosensitized inactivation of bacteriophages. Salmonella phage P22 is exponentially inactivated in the presence of 9-aminoacridine (9AA) and white light, if the particles are preincubated with 9AA. The rate of inactivation is dependent on a high order of the 9AA concentration. Mutations do not accumulate among the surviving phage.

The inactivated phage particles adsorb to bacteria but do not kill them. Marker rescue experiments with coinfecting phage reveal that the inactivated particles are unable to inject their DNA into the host cell. This phenotype is shared by P22 particles which are missing either of two minor structural proteins of the phage, gp16 or gp20.

Using SDS gel electrophoresis we have examined the proteins of the inactivated phage particles. The DNA injection proteins, gp16 and gp20, decrease in mobility with time of irradiation. The altered mobilities follows the kinetics of inactivation. This damage to the proteins does not occur in particles lacking DNA, thus the protein damage is probably mediated by 9AA bound to DNA. The DNA itself however does not show gross damage. Recovery of DNA from inactivated and control phage is the same, as are the EcoRI restriction fragment patterns.

All these data are consistent with a model in which 9AA binds to a region of the chromosome also occupied by the proteins gp16 and gp20. Absorption of a photon results in the generation of singet oxygen or other reactive species which damages the bound proteins, preventing DNA injection. The protein damage may be due to internal crosslinking within the target polypeptide chains.

M-PM-G3 LASER FLASH PHOTOLYSIS STUDIES OF ENZYME INACTIVATION. L.I. Grossweiner, Biophysics Laboratory, Physics Department, Illinois Institute of Technology, Chicago, IL 60616.

Previous work has shown the photoionization of exposed aromatic residues is a major initial process in enzymes, leading to tryptophanyl and/or tyrosinyl radicals. The ejected electrons are localized in the medium as e^-_{aq} and trapped at cystyl bridges in certain cases[1]. Laser flash measurements at 265 nm provide the initial product yields which may be compared to residue destruction and inactivation quantum yields. The results lead to the inactivation mechanisms: hen lysozyme, photolysis of Trp 62 or Trp 108[2]; carboxypeptidase A, photolysis of Trp 73 mediates zinc release[3]; ribonuclease A, photolysis of essential cystine[4]. Detailed analysis of e^-_{aq} decay kinetics indicates back reactions with the damaged enzyme competes with scavenging by undamaged molecules. The contribution of the latter to inactivation may be evaluated from pulse radiolysis where e^-_{aq} is generated in the medium. The intermolecular process constitutes a parallel UV inactivation pathway, dependent upon the e^-_{aq} sensitivity of the enzyme, the enzyme concentration, and the presence of oxygen and other e^-_{aq} scavengers.

1.Grossweiner, L.I., A.G. Kaluskar, and J.F. Baugher. (1976) Int.J. Radiat.Res. 29, 1.
2.Baugher, J.F., L.I. Grossweiner, and J.Y. Lee (1977) Photochem.Photobiol. 25,305.
3.Lee, J.Y. and L.I. Grossweiner (1978) Photochem.Photobiol. 27, 635.
4.Baugher, J.F. and L.I. Grossweiner. (1978) Photochem.Photobiol. 28, 175.

Supported by the U.S. Department of Energy under Contract EY-76-02-2217.

M-PM-G4 SIZE DETERMINATION OF ENZYMES BY RADIATION INACTIVATION. E. S. Kempner and Werner Schlegel*, National Institutes of Health, Bethesda, MD 20014.

Radiation inactivation of dry enzymes can be analyzed to give the size of the functional unit. A great advantage of this technique is that it works well with crude preparations and dried cells. However, the target molecular weights reported in the 1950's and 1960's were often considerably smaller than those obtained by contemporary biochemical techniques and this method passed from favor. The detailed knowledge of protein structure which is now available is compared with the old radiation target sizes for 37 different enzymes. It is shown that with a single exception the functional units correspond either to the entire enzyme molecule or to polypeptide subunits. The remaining eight enzymes previously studied by radiation inactivation have not been successfully purified for conventional molecular weight determinations; the predicted functional unit sizes will be shown.

The method works best with X-rays, gamma-rays and fast electrons - types of radiation that deposit energy randomly throughout the volume of the sample. The action of protons, deuterons, alpha particles and heavy ions is more complicated and target analysis is not always straightfoward.

The variation of radiation sensitivity with temperature has been reported for seven different enzymes. Analysis of these data reveals a common factor:

$$D_{37}(-100°C) = 2.57\ D_{37}(+30°C)$$

This empirical factor can be used to correct inactivation results obtained at -100°C for the temperature effect.

M-PM-G5 THE FUNCTIONAL UNIT OF POLYENZYMES: DETERMINATION BY RADIATION INACTIVATION. E. S. Kempner, J. H. Miller, W. Schlegel* and J. Z. Hearon*, National Institutes of Health, Bethesda, MD 20014.

Multifunctional enzyme systems are widely present in cells either as organelles or as smaller molecular clusters. The close proximity of sequential enzyme surfaces allows for enhancement of the overall reaction rate of the pathway and also offers new mechanisms for regulation. The detailed structure of these units is difficult to obtain because of their sensitivity to proteases and other degradative factors. A powerful technique of molecular analysis which is insensitive to non-functional impurities is target theory. It denends on the destruction of enzymatic activity by ionizing radiation. The radiation-sensitive target is a measure of the minimal combination of polypeptide chains required for the measured function. We have determined the sizes of the functional units for different enzymatic activities on the "arom" conjugate from Euglena - a polyenzyme catalyzing five sequential reactions in the shikimic acid pathway - and on two conjugates from E. coli carrying both aspartokinase and homoserine dehydrogenase activities. For all three conjugates the sizes of the functional units of different activities on one conjugate were identical. When compared to the molecular weights obtained by other techniques the functional unit size matched either the entire conjugate (aspartokinase-homoserine dehydrogenase conjugates I and II) or half the unit ("arom" conjugate). The results of this study give insight into the structural assembly of these polyenzymes. The information was obtained with minimal perturbation of the complexes and sparing laborious purification and reconstitution experiments.

M-PM-G6 THERMAL INHIBITION OF MMS INDUCED STRAND BREAK REJOINING IN CHICK CELLS. B. V. Bronk, J. D. Patton*, and D. N. Mellard*, Clemson Univ., Clemson, S. C. 29631

Early passage (1-8) chick embryo fibroblasts are found to grow equally well in monolayer culture at temperatures of 37°C or 42°C (pH~7.4), with doubling times in the range 20-35 hours. Single strand breaks measured by alkaline sucrose gradient sedimentation appear in the DNA of these cells after treatment with methyl methanesulfonate at 42°C for 1 hour at concentrations less than 1 mM. Cells were rinsed and incubated in medium after treatment at various temperatures for from one to several hours in order to study kinetics of MMS induced strand break rejoining. Rejoining occurred at 37°, 42°, and 42.5° but not at temperatures above 43°C. This is in contrast to human skin cells which grow well and rejoin these strand breaks at 37° but neither grow nor rejoin strand breaks at 42°C or above.[1]

1. Bronk, B. V., Wilkins, R. J. and Regan, J. D. (1973) Biochem. Biophys. Res. Comm. 52,1064.

M-PM-G7 CELL SURVIVAL VS. LET: A NEW TECHNIQUE OF MICROIRRADIATION.
W.C. Parkinson, J. Bardwick*, F.L. Vaughan*, The Univ. of Michigan, Ann Arbor, Mich. 48109.

Preliminary results have been obtained for the survival of mouse L-cells in which 8.7 keV/μm was deposited by charged particles using a technique that permits the determination of the energy deposited in a given cell, where in the cell it was deposited, and the subsequent fate of that cell. While the technique has now been developed to permit the location of the energy deposit to 1.0μm for 99% of the particles, for the "poor geometry" data reported here only 50% of the particles fell within 4μm. The results are: 84% of "hit" cells died within three mitotic cycles compared to 24% for "non-hit" cells, 5% of hit cells divided compared to 30% for non-hit cells, and 11% of hit cells continued to live without dividing compared to 45% of non-hit cells. These results are in disagreement with earlier work. Possible reason for the disagreement will be discussed.

M-PM-G8 ABSTRACT TRANSFERRED

M-PM-G9 ULTRAVIOLET-LIGHT INDUCED TRANSFORMATION OF HUMAN CELLS. B. Sutherland, R. Oliver*, A. Gih* and J. S. Cimino*, Department of Biology, Brookhaven National Laboratory, Upton, N.Y. 11973.

We have developed a system for ultraviolet-light induction of transformation of normal human embryonic fibroblasts to anchorage-independent growth. The procedure involves multiple ultraviolet exposures and growth under "permissive" conditions (on a plastic surface) before plating under selective conditions (in soft agar). Plates are scored for clumps, allowed to grow for 14 days, then clones are counted. The frequency of transformation increases with uv exposure up to about 10 J/m^2, then declines. The frequency of transformation declines with increasing passage number of the cells. Resulting transformants can be removed from the agar and grown on plastic surfaces; they do not show density-dependent growth control, but rapidly show crossing and piling-up of cells to form three-dimensional structures. The capacity for anchorage-independent growth seems to be unstable and segregates out during growth of the clone. The cells show prolonged (but not infinite) life in culture in comparison to non-transformed paired cultures. They are free of mycoplasma contamination and show human lactate dehydrogenase isozyme patterns. The characteristics of the transformation process and the resulting transformants are reported.
(Research carried out at Brookhaven National Laboratory under the auspices of the U.S. Department of Energy, and in part by National Institute of Health grant # CA23096 and Research Career Development Award 5K04CA00466-04 of the National Cancer Institute to BMS.)

M-PM-G10 LETHAL AND MUTATIONAL EFFECTS OF NEAR UV ON HAEMOPHILUS INFLUENZAE. E. Cabrera-Juaréz* and J. K. Setlow, Brookhaven National Laboratory, Upton, NY 11973.

Mutation and inactivation of *H. influenzae* have been measured following irradiation at various near UV wavelengths. Inactivation takes place most readily at 334 nm and drops off steeply at longer wavelengths. Mutants deficient in excision or postreplication repair show the same sensitivity to killing as the wild type. No induced mutations to resistance to novobiocin or streptomycin or to ability to utilize protoporphyrin instead of hemin were detected in the wild type at any of the wavelengths used. There were also no detectable induced mutations in an excision-defective strain after 334 nm irradiation. These results are in contrast to the *in vitro* mutation of purified transforming DNA we previously observed (Mutation Res. 35 (1976) 199-206). Our explanation of these phenomena is that in the cell but not in the purified DNA preparations there are photodynamic compounds that upon irradiation cause the formation of lethal but nonmutagenic lesions. The premutational lesions that cause mutations in transforming DNA are mostly in cells that are killed by photodynamic action.

This research was carried out at the Brookhaven National Laboratory under the auspices of the U.S. Department of Energy. Dr. Cabrera-Juárez was partially supported by a fellowship from the Dirección de Especialización Docente e Investigación Científica y Technológica, subordinate of the COFAA of the I.P.N., and by the CONACYT.

M-PM-G11 ENHANCED SURVIVAL OF HERPES SIMPLEX VIRUS GROWN ON CV-1 CELLS. EFFECT OF UV, 8-MOP, AND CELL "AGE". T. Coohill, S. Moore*, and L. James*, Western Kentucky University, Bowling Green, KY 42101.

The effects of various cellular conditions on enhanced survival of irradiated herpes simplex virus type I were studied. AGMK cells (CV1-TC7) were used to assay viral titre. This enhancement [often called Weigle Reactivation] is affected by UV exposure to the cells, the time delay between cell exposure and viral inoculation, the photosensitizing drug 8-methoxypsoralen, and cell culture "age" as measured by cell passage number. Action spectra for both the UV and the 8-MOP effects have been obtained. The "aging" effect was studied over a range of 50 cell passages. These studies were supported by FDA Contract # 223-74-6067.

M-PM-G12 HELA CELL VARIANTS WITH ALTERED RESPONSE TO MONOFUNCTIONAL ALKYLATING AGENTS. R.M. Baker, W.C. Van Voorhis,* and L.A. Spencer,* Massachusetts Institute of Technology, Cambridge, Mass. 02139.

We have identified lines of HeLa cells that display different sensitivities to EMS cytotoxicity and have examined cross-resistance and mutagenesis of these cells. Initially, we observed that a standard strain of HeLa S3 is approximately 8-fold more sensitive than the CCL2 HeLa strain of the American Type Culture Collection. Conversely, a subclone of the CCL2 strain that was sampled was found to be about 7-fold more sensitive to EMS than the parental line. In order to select single-step variants for this trait, we plated the relatively sensitive S3 line in the presence of EMS and isolated colonies appearing at very low survival. One such clone, designated A6, shows about 7-fold greater resistance to EMS killing than the S3 parent. This A6 isolate is cross-resistant to other monofunctional alkylating agents, exhibiting about 4-fold increased resistance to MMS and about 20-fold increased resistance to MNNG, but it does not differ from the S3 parent in its responses to mitomycin C, ultraviolet radiation, or γ rays. In contrast to results for cytotoxicity, the resistant A6 line showed a dose-response similar to that of S3 cells when tested for EMS induction of ouabain-resistant mutants, indicating that it does not differ from the parent with respect to susceptibility of the genome to EMS mutagenesis. Presumably these cell lines differ in their ability to repair potentially inactivating alkylating products in the DNA, but then other lesions must be responsible for most premutational damage. Thus, our results are consistent with chemical evidence that different alkylation products may be involved in mutation and inactivation (Lawley, Mutat.Res. 23, 283, 1974). Variants differing in response to alkylation have not been documented previously in cultured mammalian cells. (Supported by NIGMS and NCI).

M-PM-G13 ESTIMATION OF GENETIC RELATEDNESS AMONG BACTERIOPHAGES BY MEANS OF HIGH RESOLUTION THERMAL DENATURATION PROFILES. A. T. Ansevin, D. L. Vizard, and M. Mandel, Department of Physics and Department of Biology, University of Texas System Cancer Center, M. D. Anderson Hospital and Tumor Institute, Texas Medical Center, Houston, TX 77030.

The use of DNA thermal denaturation for taxonomic classification can be substantially improved over the earlier practice of determining just the Tm of the melting transition. In the high resolution method of denaturation far more information is acquired so that DNA mass fraction as a function of base composition can be presented over the full range of sequences present in the genome. When profiles of this type are normalized to an area proportional to the molecular weight of the DNA, the overlap of area between two derivative curves can be taken as an estimate of the potential relatedness of the DNA sequences. This technique has been applied in the examination of a series of temperate B. subtilis bacteriophages that represent four different immunity groups. Both on the basis of melting range overlap and general profile shape, the DNA of bacteriophages ρ14, ρ10, and Ø105 are judged to be related in greater than 80% of their nucleotide sequences. Overlap between ρ14 and SP16 would suggest a potential relatedness of up to 70% of the DNA, but profile shape indicates that this is an upper limit only. Profile shape and overlap show that Ø3T and ρ11 are closely related (>90%) but distantly related to the ρ14 family of phages (ca. 35% common composition). Bacteriophage SP02 has a quite different arrangement of DNA sequences from any of the others examined, as judged by profile shape. Advantages of high resolution denaturation analysis include experimental simplicity, ease of quantitation, good qualitative characterization, and uniform weighting of results from all portions of the DNA. Conclusions are consistent with other means of examining genetic relatedness. Supported by N.I.H. Grant GM 23067.